# Discovery of the Macrocycle (9E)-15-(2-(Pyrrolidin-1-yl)ethoxy)-7,12,25-trioxa-19,21,24-triaza-tetracyclo[18.3.1.1(2,5).1(14,18)]hexacosa-1(24),2,-4,9,14(26),15,17,20,22-nonaene (SB1578), a Potent Inhibitor of Janus Kinase 2/Fms-LikeTyrosine Kinase-3 (JAK2/FLT3) for the Treatment of Rheumatoid Arthritis

Anthony D. William,* Angeline C.-H. Lee, Anders Poulsen, Kee Chuan Goh, Babita Madan, Stefan Hart, Evelyn Tan, Haishan Wang, Harish Nagaraj, Dizhong Chen, Chai Ping Lee, Eric T. Sun, Ramesh Jayaraman, Mohammad Khalid Pasha, Kantharaj Ethirajulu, Jeanette M. Wood, and Brian W. Dymock

S*BIO Pte. Ltd., 1 Science Park Road, #05-09 The Capricorn, Singapore Science Park II, Singapore 117528

**ⓢ** *Supporting Information*

**ABSTRACT:** Herein, we describe the synthesis and SAR of a series of small molecule macrocycles that selectively inhibit JAK2 kinase within the JAK family and FLT3 kinase. Following a multiparameter optimization of a key aryl ring of the previously described SB1518 (pacritinib), the highly soluble **14l** was selected as the optimal compound. Oral efficacy in the murine collagen-induced arthritis (CIA) model for rheumatoid arthritis (RA) supported **14l** as a potential treatment for autoimmune diseases and inflammatory disorders such as psoriasis and RA. Compound **14l** (SB1578) was progressed into development and is currently undergoing phase 1 clinical trials in healthy volunteers.
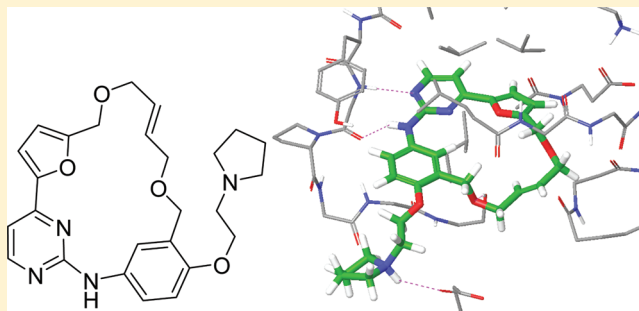
## INTRODUCTION

An estimated 1% of the world's population is afflicted by rheumatoid arthritis (RA), a chronic, systemic inflammatory disorder leading to the destruction of articular cartilage and ankylosis of the joints.[1] RA is a disabling and painful condition, which leads to substantial loss of functioning and mobility if not adequately treated. Nonpharmacological treatment includes physical, occupational, and nutritional therapy, but these do not stop the progression of joint destruction. Analgesic and anti-inflammatory drugs, including steroids, are used to suppress the symptoms, while disease-modifying antirheumatic drugs (DMARDs), such as methotrexate, hydroxychloroquin, and sulfasalazine, modify the underlying immune process in an effort to prevent long-term damage.[2] Although many patients derive benefit from DMARDs, few achieve remission, and there are many adverse events related to the liver, bone marrow, and renal toxicity, allergic skin reactions, autoimmunity and infections. More recently, the advent of biological agents targeted at pro-inflammatory cytokines, such as the anti-TNFα drugs etanercept, infliximab, and adalimumab, have successfully suppressed inflammation in many individuals with rheumatoid arthritis (RA).[3] However, these and other biologics are expensive drugs with significant side effects, and the majority of patients relapse when treatment is withdrawn.[4]

Inhibition of protein kinases implicated in cytokine signaling networks has emerged as a potential new treatment paradigm for RA.[5] The hematopoietin family of cytokines, which includes several postulated to have roles in RA (e.g., interferons, IL-2, IL-6, IL-7, IL-12, and IL-15), bind to Type I and II cytokine receptors and signal through the janus kinase-signal transducer and activator of the transcription (JAK-STAT) pathway.[6] There are 4 members of the JAK kinase family (JAK1, JAK2, JAK3, and TYK2 (tyrosine kinase 2)) which play essential roles in several important physiological processes such as hematopoiesis and lipid homeostasis.[7] JAK inhibitors with a range of selectivity profiles have been described with many now in clinical trials for treatment of various cancers (JAK1/2) and for immunosuppressive disorders (JAK3).[8−17] However, the immunosuppressive effects of inhibiting JAK3 may cause severe combined immunodeficiency syndrome (SCID); hence, targeting selected JAK proteins is thought to be desirable. JAK2 plays an essential role in the signaling of pro-inflammatory cytokines involved in the pathogenesis of RA.[18] Hence, JAK2 specific inhibitors may be differentiated from other JAK inhibitors and produce therapeutic benefits in inflammatory autoimmune diseases without immunosuppression. TYK2 is involved in Type I IFN signaling,
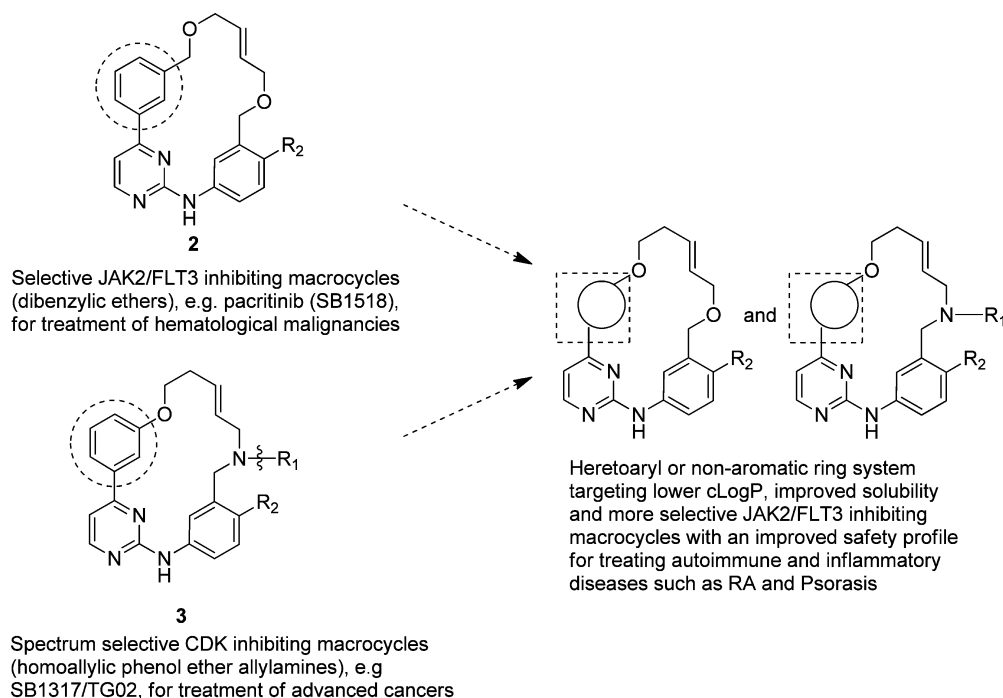
**Figure 1.** Modulating the macrocycle phenyl ring system.

and mice with a mutation in TYK2 have reduced susceptibility to collagen-induced arthritis.[19] FLT3 (fms-like tyrosine kinase 3), a class III receptor tyrosine kinase, has been implicated in RA through high levels of expression of FLT3-ligand at the site of inflammation in RA patients.[20] In a mouse antigen-induced arthritis (AIA) model treatment with the FLT3 inhibitor sunitinib reduced the intensity of synovitis and the incidence of bone destruction.[21]

Given the above evidence for therapeutic intervention via blockade of kinase signaling pathways implicated in RA, a specific JAK2/FLT3/TYK2 antagonist may have therapeutic potential.

We have recently reported the discovery of pacritinib (SB1518, (**2**, where $R_2$ = N-pyrrolidinylethoxy, Figure 1), a unique macrocyclic JAK2/FLT3/TYK2 inhibitor currently in clinical development for myelofibrosis, lymphoma, and other cancers,[22] and SB1317/TG02 (**3**, $R_1$ = Me, $R_2$ = H), a CDK/JAK2/FLT3 inhibitor for the treatment of advanced leukemias and multiple myeloma.[23] Herein, we describe the discovery of a further series of macrocycles targeting JAK2, FLT3, and TYK2 kinases, a compelling profile for the treatment of rheumatoid arthritis (RA).

**Chemistry.** We were inspired to continue to evolve the macrocycle theme aiming to develop a compound with higher selectivity, particularly against JAK3, a higher therapeutic window for nononcology applications, and improved solubility (lower cLogP), hence improving and differentiating from the first generation series.[22] We set ourselves the challenge of fine-tuning various aspects of both series described above, searching for a higher selectivity for JAK2 within the janus kinase family, while achieving our solubility goals. We set out to explore a wide range of heterocyclic rings, both saturated and unsaturated, as well as, monocyclic and bicyclic, in the biaryl-pyrimidine system (Figure 1).

Synthesis of the macrocycles via the Ring Closing Metathesis (RCM) reaction pioneered by Grubbs was carried out as previously reported employing either Grubbs second generation catalyst (($C_{46}H_{65}Cl_2N_2PRu$), [1,3-bis(2,4,6-trimethyl-phenyl)-2-imidazolidinylidene]dichloro(phenylmethylene)-

(tricyclohexylphosphine)ruthenium), or Zhan-1B catalyst (($RuCl_2[C_{21}H_{26}N_2][C_{12}H_{17}NO_3S]$), 1,3-Bis(2,4,6-trimethyl-phenyl)-4,5-dihydroimidazol-2-ylidene[2-(isopropoxy)-5-(N,N-dimethylaminosulfonyl)phenyl]methylene ruthenium(II) di-chloride).[24,25] Most products were isolated as predominately trans isomers, with a minority as inseparable mixtures of geometrical isomers. Schemes 1 and 2 illustrate the synthetic routes for construction of the left-hand and right-hand fragments, respectively.

Herein, we have introduced both saturated and unsaturated ring systems to the left-hand fragments: commercially available 2,4-dichloropyrimidine (**1a**) reacted readily with 4-piperidine-methanol under mild basic conditions to afford primary alcohol **4a**. Sodium hydride-assisted displacement with allyl bromide furnished allylether **5a** (Scheme 1). Suzuki coupling of **1a** with heterocyclic boronic acids or esters **3a–h** gave rise to a diverse range of intermediates. Indolylpyrimidines **4b** and **4q** were subsequently alkylated with either 4-bromo-1-butene, giving **5b**, or allyl bromide to give **5c** and **5j**. Thiophenes **4h** and **4j**, furans **4c**, **4l**, and **4n**, and 3-pyridyl **4f** aldehyde Suzuki products were readily reduced to alcohols by sodium borohydride, and alkylation of the alcohols was achieved under phase transfer conditions with allyl bromide, giving allylethers **5d–i** in moderate to good yield (Scheme 1).

Methods for preparing right-hand fragments **10a–e** have been previously reported for analogous compounds.[22,23] Reductive amination of 3-nitrobenzaldehye (**6a**) with N-methyl-allylamine followed by tin chloride reduction of the nitro group gave aniline **10a**. In a similar reduction/allylation/reduction sequence, **10b** was formed from **6b** following an initial alkylation with bromoethylmethyl ether. Alternatively, alkylation of **6b** with 1,2-dichloroethane gives versatile intermediate **6d**, which was reductively aminated, as for **8a**, then aminated with pyrrolidine before nitro reduction to furnish **10c**. Allylation of **7a** gave **9a** in moderate to good yield, followed by nitro reduction to give anline **10d**. Facile reduction of **6d** to **7d** followed by allylation, pyrrolidine displacement, and nitro reduction furnished aniline **10e** (Scheme 2).

**Scheme 1**[a]
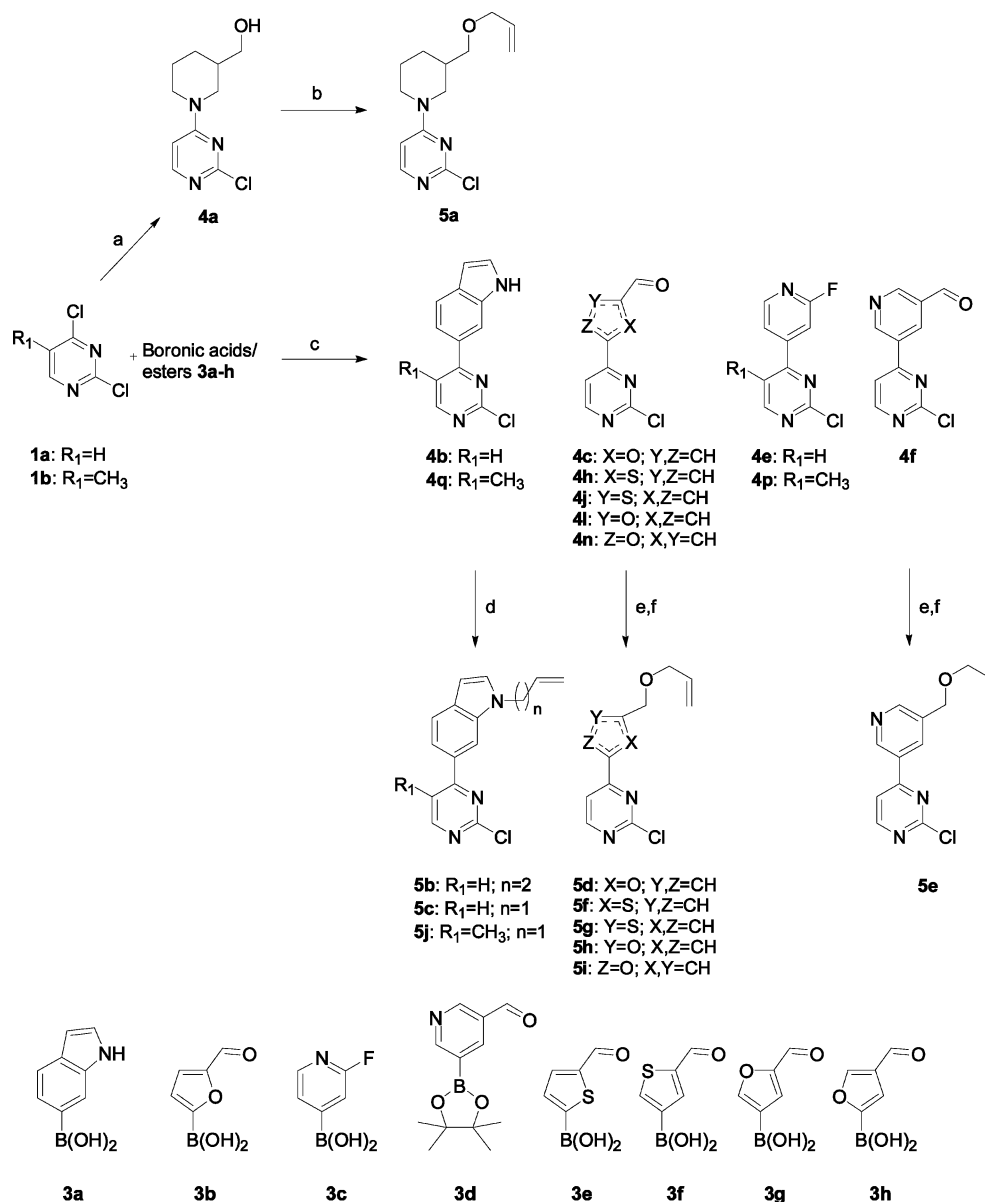


[a]Reactions and conditions: (a) 3-piperidinemethanol, Et$_3$N, CH$_2$Cl$_2$, rt, 93%. (b) Allyl bromide, NaH (60% in mineral oil), −78 °C→rt, 52%. (c) Pd(dppf)Cl$_2$·CH$_2$Cl$_2$ (1:1), Na$_2$CO$_3$, 1,2-dimethoxyethane, water, 80 °C, 58−92%. (d) 4-Bromobut-1-ene/allyl bromide, NaH (60% in mineral oil), DMF, rt, 62−77%. (e) NaBH$_4$, THF, MeOH, 0 °C, 70−94%. (f) Allyl bromide, KOH, TBAHSO$_4$, CH$_2$Cl$_2$, rt, 46−84%.

Terminal alkenes **10a−e** were coupled with the left-hand fragments **5a−j** in a high yielding acidic displacement using hydrochloric acid (Scheme 3). Ruthenium catalyzed RCM directly formed macrocycles **13a−c**, **13e−h**, **14a−d**, and **14f−n** (Tables 1 and 2). Following coupling of 2-fluoropyridyl biaryls **4e** and **4p** with **10a** and **10c**, fluoride displacement with 3-buten-1-ol, under basic conditions, produced the desired dienes in moderate yields. Macrocyclisation with Grubbs second generation catalyst, using hydrochloric acid as an additive, to neutralize the basic center, provided macrocyclic 2-pyridyl ethers **13d**, **14d**, and **14e**.

### ■ RESULTS AND DISCUSSION

**Preliminary Study of Heterocycle−Linker Combinations.** Linkers of 8 atoms in length between the meta positions of both aryl groups 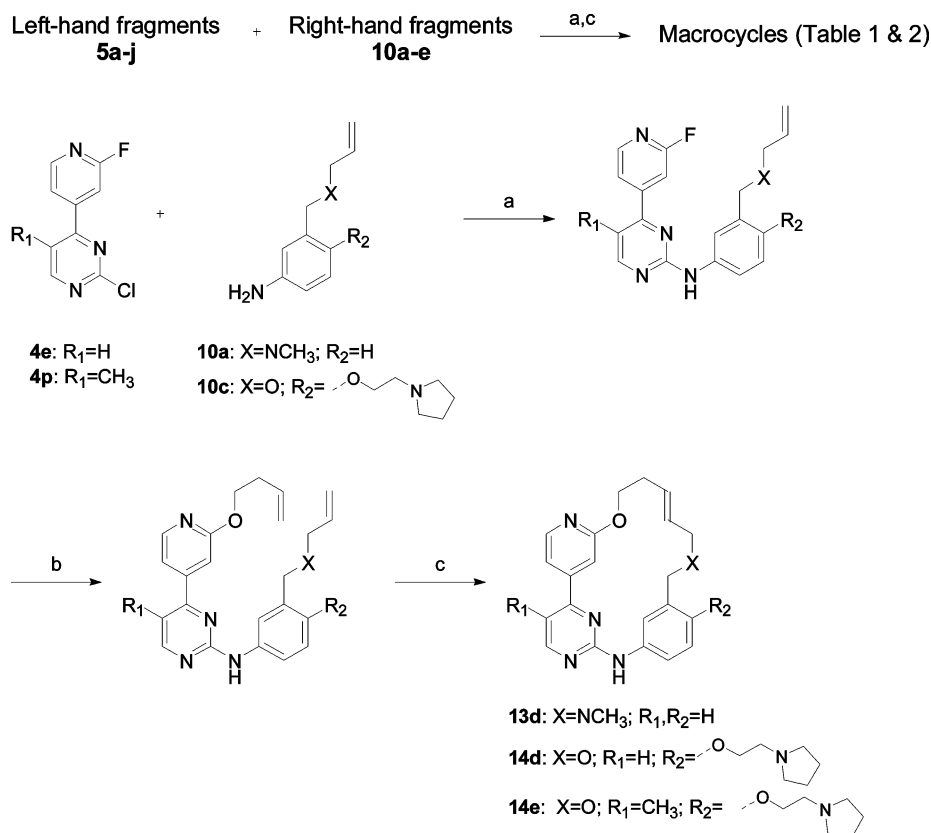were previously found to be optimal in a series of phenyl-pyrimidine compounds.[22] A selection of those linkers combined with (i) saturated; (ii) 5- or 6-membered; and (iii) bicyclic heterocycles were installed in some initial exploratory compounds. We rapidly lost interest in saturated compounds given the complete lack of activity of **13a**. However, other saturated series, with shorter linkers, were more active and will be reported in a future publication. Focusing on heteroaromatic rings, we decided to maintain the macrocycle ring size at either 17 or 18 atoms, which was found to be optimal for JAK2 activity in the phenyl series.[22] Incorporation of a bicyclic indole into the structure was possible with these restrictions giving **13b** and **13c**. Both compounds were potent against FLT3 and selective against JAK3, two key aspects of our target profile. However, only **13c** was potent against JAK2, the observed 10-fold JAK2 potency difference may be explained by the larger ring size of **13b** leading to some unfavorable clashes with the

**Scheme 2**[a]
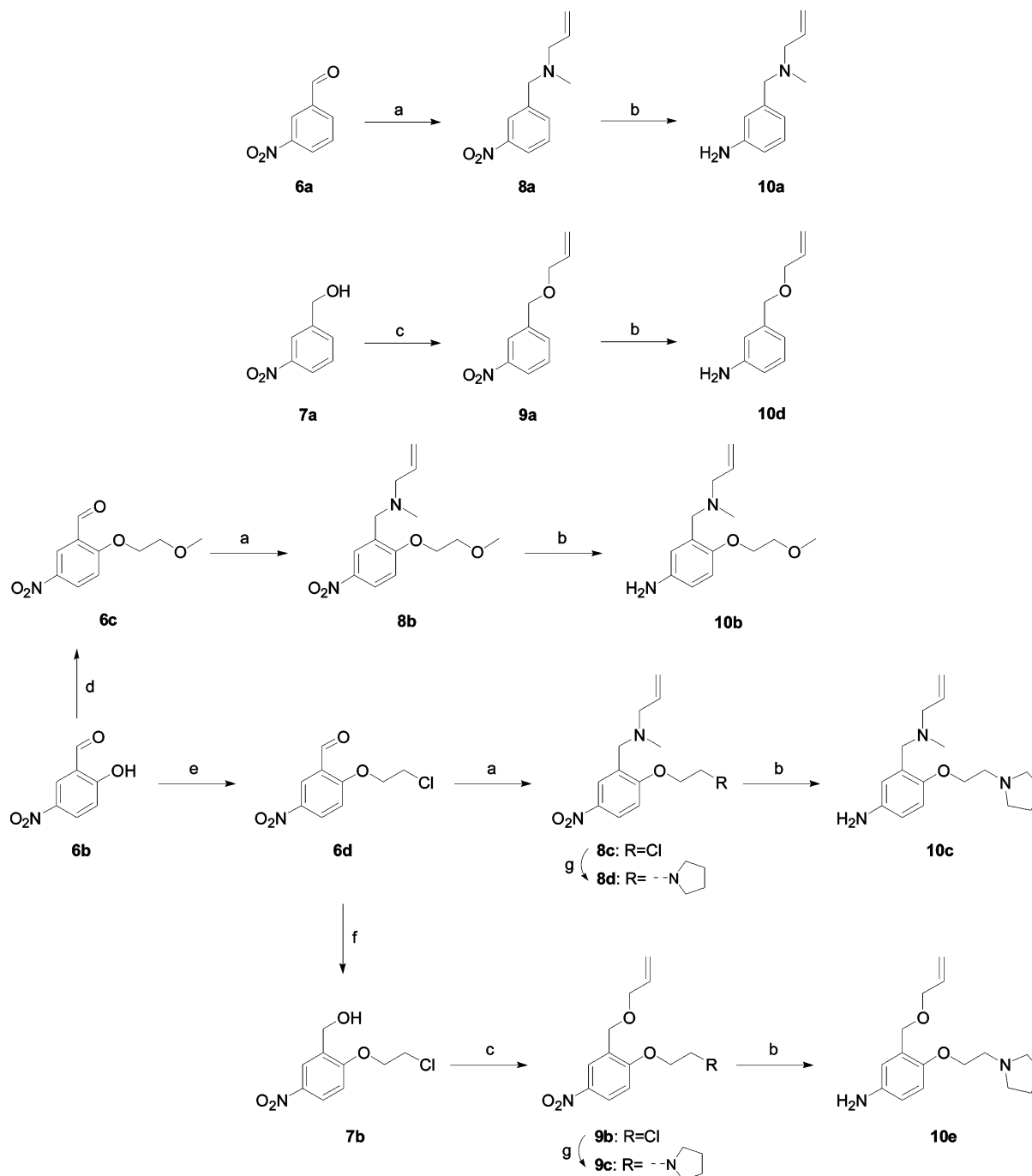


[a]Reactions and conditions: (a) N-Allylmethyl amine, Na(OAc)$_3$BH, CH$_2$Cl$_2$, rt, 75−95%. (b) SnCl$_2$·2H$_2$O, CH$_2$Cl$_2$/MeOH (1:1), rt, 64−98%. (c) Allyl bromide, KOH, TBAHSO$_4$, CH$_2$Cl$_2$, rt, 55−78%. (d) 2-Bromoethyl methyl ether, K$_2$CO$_3$, DMF, 80 °C, 86%. (e) 1,2-Dichloroethane, K$_2$CO$_3$, DMF, 100 °C, 72%. (f) NaBH$_4$, THF, water, 0 °C, 94%. (g) Pyrrolidine, DMA, 90 °C, 75−78%.

protein (Figure 2). More importantly, both compounds were active against CDK2 in the same concentration range as FLT3, a critical selectivity issue. Given this negative aspect and the generally greater challenges of synthesizing the indole macrocycles, we focused our attention on monocyclic rings. Pyridyl rings with the basic linker, such as **13d**, retained their high potency for CDK2 as expected but unfortunately lost JAK2 potency as compared to the corresponding phenyl ring (CDK2 IC$_{50}$ 0.013 μM and JAK2 IC$_{50}$ 0.073 μM).[23] CDK2 selectivity can be increased by exchanging the basic center in the linker for

an ether oxygen, as in **13e**, but surprisingly, JAK2 potency was completely abolished. This appears to be due to the placement of the pyridyl nitrogen, which is in a highly unfavorable location with regard to Asp994. Since the pyridyl is not protonated, the opportunity to interact with Asp994 is lost, and instead, a repulsive interaction forces the ligand out of the binding site (Figure 3). This is significantly reversed on changing the nature of the linker to a neutral ether group (**13f**), although selectivity for JAK1 and 3 has been achieved, CDK2 potency is high, whereas JAK2 and FLT3 activity is weak. The smaller furan ring,

**Scheme 3**[a]



4e: $R_1$=H
4p: $R_1$=CH$_3$

10a: X=NCH$_3$; $R_2$=H
10c: X=O; $R_2$=

13d: X=NCH$_3$; $R_1$,$R_2$=H
14d: X=O; $R_1$=H; $R_2$=
14e: X=O; $R_1$=CH$_3$; $R_2$=

[a]Reactions and conditions: (a) 4 M HCl, $n$-butanol, 80−100 °C, 81−86%. (b) 3-Buten-1-ol, NaH (60% in mineral oil), THF, 0 °C, 36−48%. (c). Grubbs second generation or Zhan catalyst, HCl, CH$_2$Cl$_2$, 45 °C, 36−76%.

with its hydrogens projecting externally from the macrocycle, was then explored with the same two linker types for comparison. Basic **13g** was a generally uninteresting moderately potent CDK2 inhibitor, but **13h** was much more interesting with submicromolar JAK2, TYK2, and FLT3 potency, as well as selectivity for JAK1 and 3. CDK2 potency is still a major issue (see Figure S2, Supporting Information), but we felt this series was worthy of further work to attempt to improve potency against the key targets and eliminate CDK2 activity.

**Study of Heterocycle−Linker Combinations with Solubilizing Side Chains.** From our earlier work,[22] we had identified a robust solubilizing side chain which conferred good JAK2 and FLT3 potency as well as physicochemical properties. Given the similarities between this reported series and the heterocyclic series discussed herein, we decided to install the same side chain in a selection of heterocyclic macrocycles from Table 1 to understand if the same benefits were transferred. Adding the preferred side chain to **13c** gave **14a**, which did experience a slight improvement in JAK2 potency; however, its FLT3 potency was increased by an order of magnitude giving a single digit nanomolar IC$_{50}$ (Table 2). Although CDK2 potency of **14a** dropped by 3-fold, JAK3 potency had become significant. Addition of a 5′-methyl group to the pyrimidine ring has been previously found to boost JAK2 (and, undesirably, JAK3) potency in the phenyl series.[22] However, when the same change is installed in the indole, giving **14b**, JAK2 potency is actually reduced, and surprisingly, JAK3 activity is abolished. CDK2 potency of **14b** dropped by 10-fold compared to that of **14a**, but the high cLogP and disappointing JAK2 activity prompted us to move our focus to monocyclic rings.

Comparing 3-pyridyl **14c** with **13f**, we observed a trend similar to that of the indole series: a modest improvement in JAK2 potency, good FLT3 activity, and much improved CDK2/JAK2 selectivity. However, JAK3/JAK2 selectivity had dropped significantly. In general, 3-pyridyl compounds do not benefit fully from the addition of the pyrrolidinylethoxy side chain most likely due to repulsive forces between the unprotonated lone pair and amino acid residues (Figure 3). However, this is not the case with the 4-pyridyl compounds typified by **14d**, which has an IC$_{50}$ of 18 nM against JAK2. In addition, **14d** has good activity against TYK2 and FLT3 and over 10-fold selectivity for CDK2 and over 50-fold selectivity for JAK1 and JAK3. The direct comparator without the side chain was not prepared, but clearly this profile is much improved over **13d** and moving toward our target profile. As discussed above for **14b**, previous studies had shown that a 5′-methyl pyrimidine group could boost JAK2 potency. When **14e** was prepared and tested, we found that JAK2 potency remained unchanged, but we were pleasantly surprised to see much increased selectivity for CDK2 (CDK2/JAK2 = 278-fold for **14e**); however, the extra methyl had increased cLogP to 4.8. For this reason, we did not extend the study of the 5′-pyrimidyl substituents. Such good potency of pyridyl analogues **14d** and **14e** may be explained by a potential water-mediated H-bond to Asp981 (Figure 4).

5-Membered heterocycles were also investigated with the preferred pyrrolidinyl-ethyloxy side chain. Furan and thiophene analogues **14f** and **14g** with the basic N-methyl linker were moderately potent against JAK2 but the latter exhibited good activity for TYK2 and FLT3. An alternative side chain,

## Table 1. SAR of Macrocycles with Hetero-Atomic Ring Bi-Aryl to Pyrimidine

| Cpd[a] | Structure | CDK2 IC$_{50}$ (μM)[b] | JAK1 IC$_{50}$ (μM)[b] | JAK2 IC$_{50}$ (μM)[b] | JAK3 IC$_{50}$ (μM)[b] | FLT3 IC$_{50}$ (μM)[b] | TYK2 IC$_{50}$ (μM)[b] | cLogP |
|---|---|---|---|---|---|---|---|---|
| 13a | | >10 | >10 | >10 | >10 | >10 | >10 | 3.5 |
| 13b | | 0.077±0.0 | 1.0±0.13 | 1.6±0.071 | >10 | 0.093±0.00 | 1.5±0.14 | 4.8 |
| 13c | | 0.083±0.024 | 4.8±0.071 | 0.15±0.014 | >10 | 0.073±0.033 | 0.15±0.035 | 4.8 |
| 13d | | 0.022±0.0021 | 0.17±0.0071 | 0.26±0.0 | >10 | 0.31±0.0071 | 0.065±0.0042 | 3.8 |
| 13e | | 0.42±0.085 | >10 | >10 | >10 | 4.8±0.0 | 5.9±1.1 | 2.6 |
| 13f | | 0.20±0.035 | >10 | 0.93±0.042 | >10 | 0.56±0.028 | 0.95±0.071 | 3.1 |
| 13g | | 0.32±0.0 | 1.8±0.14 | 0.82±0.064 | >10 | 0.77±0.22 | 1.5±0.071 | 3.1 |
| 13h | | 0.68±0.11 | 8.0±0.071 | 0.22±0.014 | >10 | 0.62±0.0 | 0.67±0.064 | 3.4 |

[a]All compounds were isolated as c.95:5 trans/cis mixtures. [b]All IC$_{50}$ values are the mean ± SD of at least two independent experiments.

methoxyethoxy (compounds **14h** and **14i**), showed that the pyrrolidine enhances JAK2 potency by 3–5-fold (compare **14f** with **14h** and **14g** with **14i**). Again, as for **14f** and **14g**, the thiophene was more active than furan. This may be explained by the highly lipophilic nature of the binding site where the thiophene is interacting (Figure S1, Supporting Information). Significant JAK2 potency gains were achieved with the combination of thiophene, diether linker, and pyrrodine side chain: **14j** exhibited a JAK2 IC$_{50}$ of 7 nM with 32 and 24 nM for

TYK2 and FLT3, respectively. Furthermore, this compound was 400-, 57-, and 89-fold selective for CDK2, JAK1, and JAK3, respectively. Although cLogP was a little high, we were encouraged to progress the profiling of **14j** due to its excellent potency and selectivity profile.

When the thiophene sulfur is moved to a regioisomeric position at the exterior of the macrocycle (**14k**), the in vitro potency profile was quite similar to that of **14j**, but cLogP rises significantly. Constraints on the molecular conformation of the
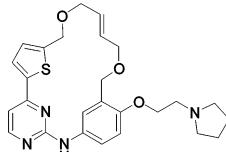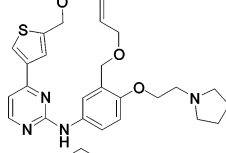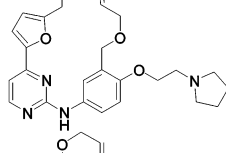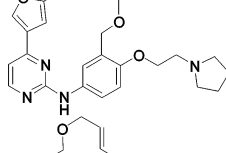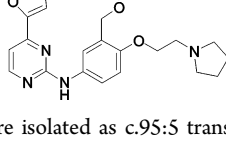
macrocycles clearly have the potential to result in significantly different physicochemistry lending another dimension to the SAR and opportunities to tune the structure to a preferred profile. The analogous furan to **14j** was less active against JAK2 (see Figure S1, Supporting Information) but did have a very positive selectivity profile: **14l** has a JAK2 IC$_{50}$ of 46 nM and selectivity of 152-, 58-, and 93-fold for CDK2, JAK1, and JAK3, respectively. Its potency against FLT3 is in the same concentration range as JAK2 with 5-fold selectivity against TYK2.

cLogP is lower for **14l** than for **14j**, but both compounds were selected for further assessment along with **14k**. Another compound selected for further profiling was **14m**, the furan comparator of **14k**. In this case, the cLogP is reduced to 3.6 with the polar oxygen atom more exposed to solvent. The overall potency profile of **14m** is similar to that of **14l** but with improved CDK2 selectivity (**14m** CDK2 IC$_{50}$ >10 $\mu$M). Moving the oxygen atom in the furan to the remaining ortho position (**14n**), with respect to the pyrimidine, results in a further drop in JAK2 and

### Table 2. SAR Study of Aromatic Ring Substitutions with Small Groups for Fine Tuning Selectivity and Solubility

| Cpd[a] | Structure | CDK2 IC$_{50}$ ($\mu$M)[b] | JAK1 IC$_{50}$ ($\mu$M) | JAK2 IC$_{50}$ ($\mu$M) | JAK3 IC$_{50}$ ($\mu$M) | FLT3 IC$_{50}$ ($\mu$M)[b] | TYK2 IC$_{50}$ ($\mu$M) | cLogP |
|---|---|---|---|---|---|---|---|---|
| 14a |  | 0.23±0.035 | nd | 0.063±0.063 | 1.14±0.28 | 0.0079±0.0011 | nd | 5.2 |
| 14b |  | 2.5±0.67 | 5.1±0.64 | 0.37±0.028 | >10 | 0.017±0.00 | 0.44±0.021 | 5.3 |
| 14c |  | 3.2±0.14 | >10 | 0.29±0.085 | 1.0±0.13 | 0.063±0.0028 | 0.63±0.028 | 3.4 |
| 14d |  | 0.27±0.059 | 0.97±0.26 | 0.018±0.0027 | 1.4±0.18 | 0.031±0.0062 | 0.030±0.003 | 4.6 |
| 14e |  | 3.9±0.66 | 0.39±0.11 | 0.014±0.0021 | 1.0±0.24 | 0.031±0.0085 | 0.072±0.012 | 4.8 |
| 14f |  | 1.6±0.49 | 0.65±0.078 | 0.33±0.050 | >10 | 0.12±0.054 | 0.71±0.014 | 3.5 |
| 14g |  | 0.71±0.42 | 0.20±0.021 | 0.090±0.0014 | >10 | 0.012±0.0028 | 0.041±0.00071 | 3.9 |
| 14h |  | 8.6±0.35 | 3.2±0.0 | 1.1±0.18 | >10 | 1.2±0.34 | 0.59±0.014 | 3.4 |
| 14i |  | 0.33±0.0 | 0.39±0.014 | 0.17±0.028 | >10 | 0.022±0.001 | 0.033±0.0042 | 3.8 |

**Table 2. continued**

| Cpd[a] | Structure | CDK2 IC$_{50}$ ($\mu$M)[b] | JAK1 IC$_{50}$ ($\mu$M) | JAK2 IC$_{50}$ ($\mu$M) | JAK3 IC$_{50}$ ($\mu$M) | FLT3 IC$_{50}$ ($\mu$M)[b] | TYK2 IC$_{50}$ ($\mu$M) | cLogP |
|---|---|---|---|---|---|---|---|---|
| 14j | | 2.9±0.81 | 0.42±0.12 | 0.0073±0.0016 | 0.65±0.17 | 0.024±0.0061 | 0.032±0.0085 | 4.1 |
| 14k | | 6.8±0.35 | 1.5±0.14 | 0.017±0.0035 | 0.68±0.17 | 0.045±0.018 | 0.047±0.0 | 4.6 |
| 14l | | 7.0±2.0 | 2.7±0.81 | 0.046±0.0067 | 4.3±1.8 | 0.060±0.013 | 0.23±0.046 | 3.9 |
| 14m | | >10 | 3.0±0.49 | 0.067±0.0071 | 8.8±0.57 | 0.048±0.014 | 0.12±0.0071 | 3.6 |
| 14n | | >10 | 1.9±0.21 | 0.11±0.0 | 9.2±0.21 | 0.18±0.023 | 0.31±0.021 | 3.7 |

[a]All compounds were isolated as c.95:5 trans/cis mixtures. [b]All IC$_{50}$ values are the mean ± SD of at least two independent experiments.
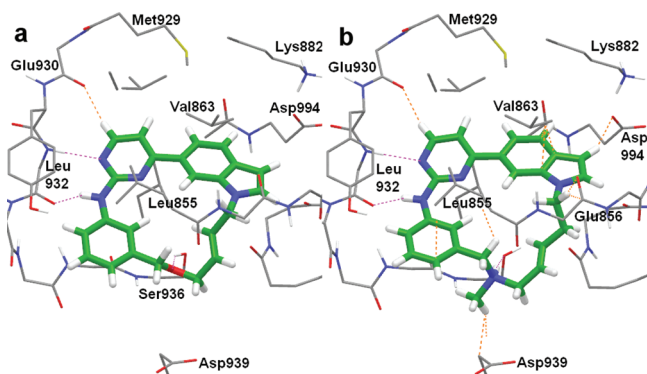


**Figure 2.** (A) Compound **13c** docked into JAK2. Hydrogen bonds are shown in magenta dashed lines and close contacts in orange dashed lines. The only close contact between **13c** and JAK2 is between the backbone carbonyl of Glu930 and the free hydrogen next to the pyrimidine nitrogen of **13c**. This is an attractive interaction and may be described as a weak hydrogen bond. (B) Compound **13b** docked into JAK2. The macrocyclic linker of **13b** is more bulky than that of **13c**, and consequently **13b** has several close contacts to the protein. The reduced JAK2 activity of **13b** may be due to slight clashes with the protein.



**Figure 3.** Sitemap analysis of JAK2 with **13e** docked into the ATP-binding site. White dots indicate positions where it is favorable to place ligand atoms. The yellow, blue, and red grids are hydrophobic and hydrogen bond acceptor and donor areas of the binding site, respectively. The pyridine nitrogen falls into the hydrogen bond donor area around the carboxylic acid group of Asp994. The interaction with Asp994 will be repulsive (distance 3.7 Å) unless the pyridine is protonated. The pyridine pK$_a$ is calculated by Epik to be 3.6, which indicates it is not protonated; hence, the negative interaction of the pyridine forces the compound out of the binding site leading to a lower IC$_{50}$.

FLT3 activity below 100 nM, although the excellent CDK2 selectivity was retained.

**Further In Vitro Profiling of Selected Compounds.** Selected inhibitors which met our criteria of JAK2 and FLT3 potency with selectivity against CDK2, JAK1, and JAK3 were further profiled in vitro (Table 3). A few potent compounds
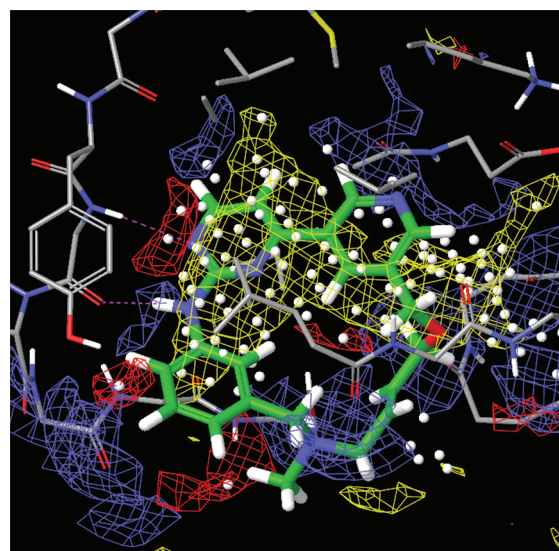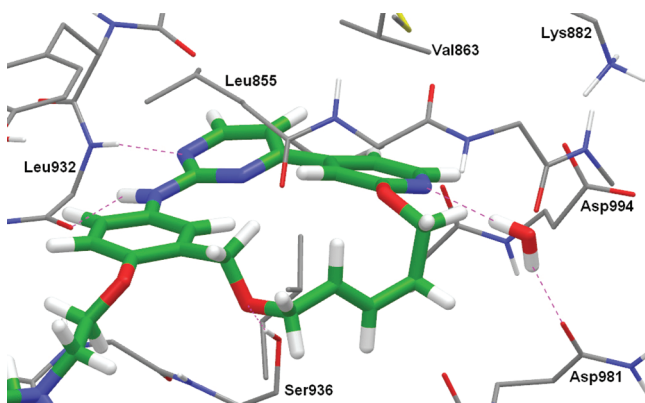
**Figure 4.** Compound **14d** docked into JAK2. There is room for a water molecule which may mediate a hydrogen bond between the pyridine nitrogen and the side chain of Asp981. This may explain the increased JAK2 activity of pyrimidine analogues like **14d** and **14e**.

with higher cLogPs (**14e** and **14k**) are compared for information purposes. Even the higher cLogP compounds had acceptable solubility, but **14l** and **14m** were superior in this important respect. CYP3A4 and 2D6 were not an issue with the tested compounds with the exception of the high cLogP **14e**, which inhibited CYP3A4 with an IC$_{50}$ of 0.97 $\mu$M. Human microsomal stabilities were remarkably good, as has been previously noted with these macrocyclic compounds. Stability was lower in mouse microsomes but still acceptable for further preclinical evaluation in mouse models. On-target cellular potency was evaluated in a cell proliferation assay using two cancer cells lines: Ba/F3 (driven by the JAK2 V617F mutant) and HL60 (driven by FLT3). Cell proliferation data (GI$_{50}$) vary about 5-fold between the selected compounds (Table 3). As a measure of cell inhibition efficiency, GI$_{50}$/IC$_{50}$ shows that **14k** and **14l** were the most efficient compounds in Ba/F3 cells (JAK2 driven) and that **14j** was the best performing compound, relative to its enzyme IC$_{50}$, in HL60 cells. Compounds **14k**, **14l**, and **14m** were similarly efficient in HL60 cells. Apart from solubility, there did not appear to be any significant differences in vitro between high and low cLogP compounds. Of the preferred lower cLogP compounds **14j**, **14l**, and **14m**, we were concerned about the metabolites of furan compounds. Furans can be metabolized to 1,4-*cis*-butendials, which are toxic.[26,27] However, it is reported that 2,5-disubstitued furans, such as ranitidine, are quite stable in vivo;[28] hence, we felt that **14l**, being 2−5-disubstituted, posed less of a risk than **14m**. Highly potent **14j** was an attractive compound from most respects but only moderately soluble. Selection of a preferred single candidate was aided by hERG screening (binding assay). In general, the pyridyl derivatives were moderately potent with IC$_{50}$s in the 1−5 $\mu$M range. We were aiming to eliminate hERG activity as a concern; hence, **14l** was preferred over **14j** (>10 $\mu$M (14% at 10 $\mu$M) and 7.2 $\mu$M, respectively). Taken together, this complex set of data supported **14l** as the preferred candidate. Although **14l** was not always the best compound in each test category, it did, however, meet our minimum target profile in all areas with a balanced compromise between the criteria. Hence, **14l** was selected as the preferred drug candidate and went forward into more advanced profiling studies.

In silico, **14l** meets all accepted drug-like guidelines for an orally absorbed small molecule with molecular weight less than 500, a cLogP less than 5, numbers of H-bond donors and acceptors less than 5 and 10, respectively, and a polar surface

**Table 3. Further in Vitro Profiling of Preferred Compounds Leading to Selection of in Vivo Candidate 14l**

| cpd | JAK2 IC$_{50}$ ($\mu$M)[a] | CDK2/ JAK2[a] | JAK1/ JAK2[a] | JAK3/ JAK2[a] | TYK2/ IC$_{50}$ ($\mu$M) | FLT3 IC$_{50}$ ($\mu$M)[a] | Solubility ($\mu$g/mL)[b] | cLogP | CYP3A4 IC$_{50}$ ($\mu$M)[a,c] | CYP2D6 IC$_{50}$ ($\mu$M)[a,c] | HLM $t_{1/2}$ (min)[d] | MLM $t_{1/2}$ (min)[d] | hERG IC$_{50}$ ($\mu$M)[g] | Ba/F3 GI$_{50}$ ($\mu$M)[a] | GI$_{50}$/ IC$_{50}$[e] | HL60 GI$_{50}$ ($\mu$M)[a] | GI$_{50}$/ IC$_{50}$[f] |
|---|---|---|---|---|---|---|---|---|---|---|---|---|---|---|---|---|---|
| 14e | 0.014 | 278 | 28 | 71 | 0.072 | 0.031 | 243 ± 5 | 4.8 | 0.97 ± 0.19 | >10 | >60 | 25 | 2 (Est.)[h] | 0.13 ± 0.036 | 9.3 | ND | ND |
| 14j | 0.0073 | 397 | 58 | 89 | 0.032 | 0.024 | 154 ± 16 | 4.1 | >10 | >10 | >60 | 27 | 7.2 | 0.055 ± 0.007 | 7.5 | 0.20 ± 0.042 | 8.3 |
| 14k | 0.017 | 400 | 88 | 40 | 0.047 | 0.045 | 218 ± 18 | 4.6 | ND | ND | >60 | 25 | ND | 0.080 ± 0.028 | 4.7 | 0.64 ± 0.049 | 14.2 |
| 14l | 0.046 | 152 | 59 | 93 | 0.23 | 0.060 | >250 | 3.9 | >10 | >10 | >60 | 27 | >10 | 0.25 ± 0.19 | 5.4 | 0.85 ± 0.34 | 14.2 |
| 14m | 0.067 | >149 | 45 | 131 | 0.12 | 0.048 | >250 | 3.6 | >10 | >10 | >60 | 18 | ND | ND | ND | 0.71 ± 0.18 | 14.8 |

[a]All IC$_{50}$ and GI$_{50}$ values are means of at least two independent experiments. [b]High throughput solubility in PBS buffered at pH 7.0. [c]CYP activity determined in the human liver microsome system, see Experimental Section for details. [d]One determination. [e]Ba/F3 GI$_{50}$/JAK IC$_{50}$. [f]HL60 GI$_{50}$/JAK IC$_{50}$. [g]Dofetalide binding, single determination carried out by MDS Pharma Services. [h]Estimated value; **14e** was not tested but pyridyl analogue **14d** had a hERG binding IC$_{50}$ of 2.4 $\mu$M as did other pyridyl analogues. ND denotes not determined.

area of less than 120 Å$^2$. Compound **14l** is highly soluble, >250 $\mu$g/mL, in the kinetic experiment and 0.88−1.43 mg/mL in the thermodynamic experiment buffered to pH 7.0. This solubility compares very well to that of **2** (where R$_2$ = $N$-pyrrolidinylethoxy, Figure 1), which is 150 $\mu$g/mL at pH 7.0. In the Caco-2 bidirectional permeability assay, **14l** showed high permeability with an efflux ratio of 1.1, which indicated that **14l** is probably not a substrate for $p$-glycoprotein in humans and thus may show high intestinal absorption. Compound **14l** was found to be stable in liver microsomal stability studies with HLM, MLM, RLM, and DLM $t_{1/2}$ > 60 min and was moderately stable in MoLM with $t_{1/2}$ of 23 min (Table 4). Compound **14l** did not

### Table 4. Physicochemical Properties and in Vitro ADME of 14l

| property | value |
| --- | --- |
| mol.wt | 463 |
| no. of HDB | 1 |
| no. of HBA | 7 |
| cLogP | 3.9 |
| log $D$ (pH 7.4) | 1.58 |
| PSA (Å$^2$) | 82 |
| thermodynamic solubility pH 7.0 (mg/mL) | 0.88−1.43$^a$ |
| permeability ($P_{app, A \to B}$, $\times 10^{-6}$ cm/sec) | 24.8, efflux ratio = 1.1 (low)$^b$ |
| liver microsomes ($t_{1/2}$, min) | >60$^c$ |
| MoLM ($t_{1/2}$, min) | 23$^d$ |
| human CYP inhibition IC$_{50}$ ($\mu$M) | >10$^e$; 1.4$^f$ |
| CYP450 phenotyping | cleared by 3A4 |
| CYP450 induction | negative for 3A4 and 1A2 |
| plasma protein binding (%)$^g$ | 99.0 (H); 98.7(Mo), 87.3−87.5 (M, R, D) |

$^a$Two determinations of two different batches of **14l**. $^b$Caco-2 bidirectional permeability assay. $^c$Human, dog, rat, and mouse. $^d$Rhesus monkey microsomes. $^e$Human CYP3A4, 1A2, 2D6, 2C9·CYP3A4, and 2D6; fluorescence detection. $^f$2C19. $^g$Equilibrium dialysis assay at 1000 ng/mL. H = human, Mo = monkey, M = mouse, R = rat, and D = dog.

inhibit the major drug metabolizing human CYP450s 1A2, 3A4, 2D6, and 2C9 at below 10 $\mu$M but did inhibit 2C19 (IC$_{50}$ ~1.4 $\mu$M), suggesting that it may not have the potential to cause drug−drug interactions in vivo. In vitro plasma protein binding of **14l** was high and similar in humans and monkeys and was significantly lower in mouse, dog, and rat plasma.

Testing against a panel of kinases revealed that **14l** is approximately 20-fold selective against a cross-section of other kinases with the exception of c-fms receptor kinase (IC$_{50}$ 69 nM) and CDK9 (IC$_{50}$ 36 nM). Elevated levels of c-fms ligand, macrophage colony stimulating factor (M-CSF), are observed in the joints of RA patients; hence, due to its pivotal role in the pathogenesis of RA, the blockade of the M-CSF/c-fms axis has been shown to inhibit the progression of arthritis.[29] CDK9 promotes RNA synthesis for cell growth and differentiation and has been identified as a potential target for therapeutic intervention in oncology, virology, and cardiology.[30]

**Pharmacokinetics of 14l in Multiple Species.** The pharmacokinetic properties of **14l** are sumarized in Table 5. Compound **14l** showed rapid to moderately fast absorption ($t_{max}$ ranged between 0.5 to ~2.3 h) in mice, rats, and monkeys and was relatively slower in dogs.

### Table 5. Oral Pharmacokinetic Parameters (Mean ± SD) of 14l in Mouse, Rat, Dog, and Rhesus Monkey

| parameter | mouse$^a$ | rat ($n$ = 3) | dog ($n$ = 3) | monkey($n$ = 3) |
| --- | --- | --- | --- | --- |
| dose (mg/kg) | 50 | 50 | 5 | 20 |
| $C_{max}$ (ng/mL) | 1227 | 231 ± 85 | 27 ± 7 | 1976 ± 575 |
| $t_{max}$ (h) | 0.5 | 2.3 ± 1.5 | 3.0 ± 1.0 | 2.0 ± 1.0 |
| $t_{1/2}$ (h) | 0.8 | 3.6 ± 1.4 | 1.5 ± 0.5 | 1.1 ± 0.3 |
| AUC$_{0-\infty}$(ng·h/mL) | 2020 | 1499 ± 192 | 96 ± 33 | 7590 ± 2958 |
| oral bioavailability (F%)$^b$ | 34 | 6 | 6 | 32 |

$^a$Estimated from mean concentration time data ($n$ = 3 mice per time point). $^b$Mean.

The terminal $t_{1/2}$ was moderate in mice, dogs, and monkeys (ranged between 0.8 and 1.5 h) and longer in rats (3.6 h). The oral bioavailability was moderate in mice and monkeys (32−34%) and poor in rats and dogs (6%). Exposures achieved in mice at 50 mg/kg exceeded the pharmacological concentrations (JAK2 IC$_{50}$ = 46 nM and FLT3 IC$_{50}$ = 62 nM).

**Modulation of JAK2 Signaling Pathways.** The effects of **14l** on JAK2 signaling were investigated in 4 different cellular contexts: a cell line expressing constitutively activated mutant JAK2 (SET2, Figure 5A);[31] a cell line expressing constitutively activated wild-type JAK2 (MDA-MB-231, Figure 5B); a cell line requiring exogenous ligand to activate wild-type JAK2 (HEK293, Figure 5C); and primary human T cells (Figure 5D). JAK2 signaling was dose-dependently inhibited by **14l** treatment in all four cell systems. Note that **14l** inhibited cell proliferation in SET2 cells with an IC$_{50}$ of 0.246 nM.

Following cell incubation with **14l**, 30 $\mu$g of cell lysates were resolved on SDS−PAGE, transferred onto PVDF membranes, and probed with the respective antibodies. (A) SET2 cells were treated with various concentrations of **14l** for 4 h. (B) MDA-MB-231 cells were treated with various concentrations of **14l** for 4 h. (C) HEK293 cells were incubated with various concentrations of **14l** for 3 h followed by treatment with 1000 U/mL IFN-$\gamma$. (D) Human CD4$^+$ T cells were incubated with various concentrations of **14l** for 3 h followed by treatment with 10 ng/mL interleukin-12.

**Treatment with 14l is Efficacious in the Murine Collagen Induced Arthritis Model.** The murine CIA model recapitulates the clinical and histological development of human rheumatoid arthritis and has been useful in evaluating the effects of clinically used agents.[32,33] After the onset of collagen induced arthritis, mice were administered twice daily with doses of 105 mg/kg or 210 mg/kg (free base equivalent) of **14l**, and the treatment was continued for 10 days. In the vehicle group, the clinical arthritic score of mice increased rapidly from day 0 to disease day 11 (Figure 6). Treatment with **14l** led to a dose-dependent inhibition of arthritis, with a 23% and 59% reduction in the AUC in the mice administered 105 mg/kg and 210 mg/kg **14l**, respectively. Treatment effects at the higher dose were comparable to the mice treated with dexamethasone with a 63% reduction in the AUC. This reduction in the clinical arthritis scores was also accompanied by substantial improvement in the histopathology of the drug-treated mice (data not shown). This data shows that inhibition of JAK2 signaling, which is involved in the pathological responses of inflammatory and autoimmune diseases, could be an efficacious new paradigm for the treatment of rheumatoid arthritis.
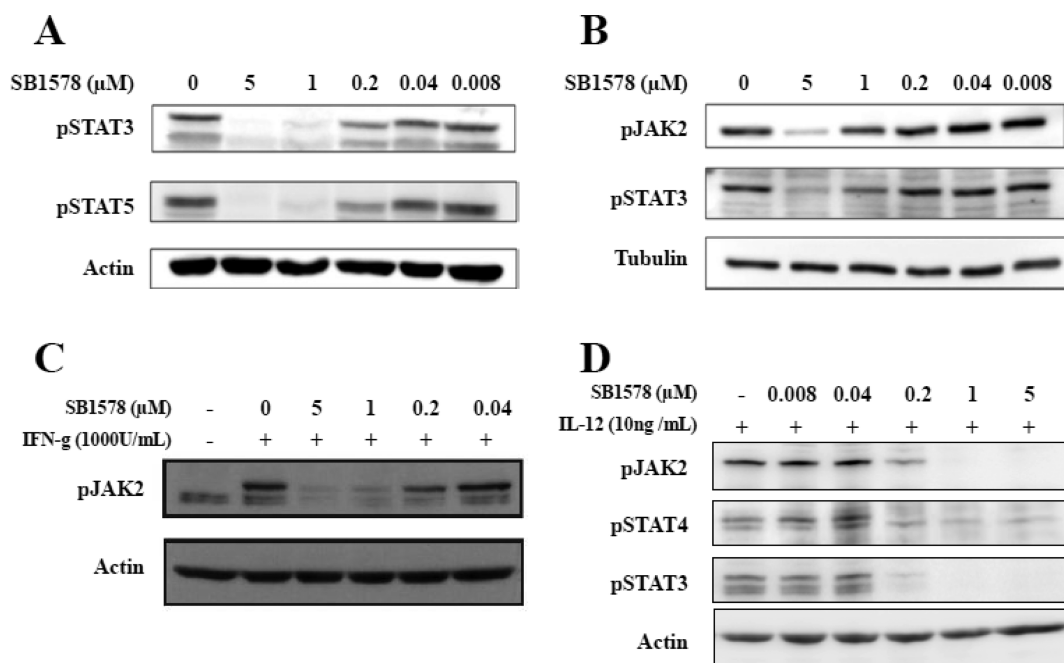
**Figure 5.** Compound **14l** blocks JAK2 signaling pathways in multiple cellular contexts.
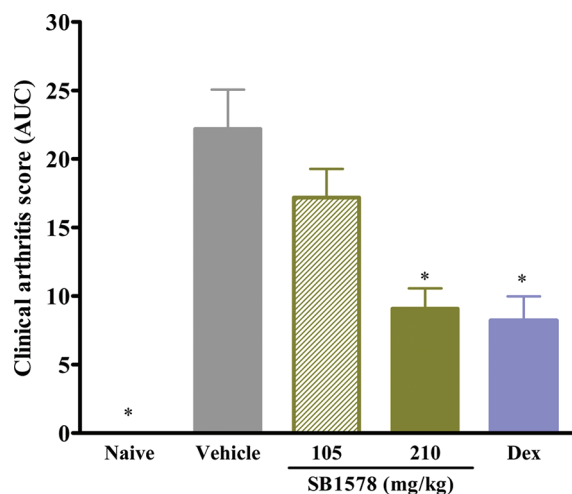


**Figure 6.** Compound **14l** attenuates clinical symptoms of arthritis in a mouse CIA model.

Arthritis was induced in mice by immunization with type II collagen emulsified in Freund's Complete Adjuvant. Following the disease onset (day 0), the mice were enrolled into treatment groups of 10 and were orally administered with **14l** (105 or 210 mg/kg b.i.d, free base equivalent) or dexamethasone (0.1 mg/kg); naïve group had 4 mice. Clinical arthritis scores were evaluated daily for 10 days. The graph represents the analysis of clinical arthritis scores with area under the dosing curve calculation, $*p \leq 0.05$, Mann−Whitney U test to vehicle.

## CONCLUSIONS

This article provides a further demonstration that conformationally constrained macrocycles can be potent and selective inhibitors of kinases. This research has general applicability to kinase inhibitors since the macrocyclic linkage is distinct from the hinge binding region of the inhibitor. Using this simple paradigm, we demonstrate that a significant degree of kinase selectivity is, in fact, achievable starting from rather unpromising N-aryl pyrimidines. Ring-closing metathesis chemistry has been successfully employed to construct relatively rigid ATP-competitive heterobiaryl macrocycles, with significantly reduced degrees of conformational freedom over typical non-macrocyclic kinase inhibitors. In addition to being potent inhibitors of JAK2, FLT3, and TYK2, this series has good physicochemical properties explaining the good translation of potency to the cell. Exchange of the previously described phenyl system[22] for heteroaryls was found to be fruitful with SAR studies leading to the 5-membered thiophene and furan rings as preferred motifs. Following extensive in vitro and in vivo profiling, highly soluble **14l**, with negligible hERG binding inhibition, was shown to inhibit its targets in cells and in vivo. Tolerable twice daily oral doses of **14l** in the mouse CIA model led to efficacy similar to that of dexamethasone; hence, **14l** was therefore selected for further development. Compound **14l** (SB1578) is currently being evaluated in phase 1 clinical trials in healthy volunteers.

## EXPERIMENTAL SECTION

**Chemistry.** Purity was >95% for all tested compounds except those indicated in their respective synthesis descriptions. For detailed HPLC analytical methods and general chemistry, refer to our earlier publication.[22]

*[1-(2-Chloro-pyrimidin-4-yl)-piperidin-3-yl]-methanol (4a).* To a solution of 2,4-dichloropyrimidine **1a** (1.86 g, 12.5 mmol), 3-piperidinemethanol (1.59 g, 13.8 mmol) in $CH_2Cl_2$ (80 mL) was added $Et_3N$ (2.0 mL, 14.4 mmol), and the resulting mixture was stirred at room temp for 2 h. Aqueous $Na_2CO_3$ was added, and the product was extracted with $CH_2Cl_2$ thrice. After workup, a solid (2.67 g; yield, 94%) was obtained as a mixture of title compound and isomer (i.e., [1-(4-chloro-pyrimidin-2-yl)-piperidin-4-yl]-methanol) in a ratio of 87:13 as determined by ${}^1H$ NMR. The crude mixture was taken forward for the next step without any further purification. The title compound (the major product): LC-MS (ESI positive mode) $m/z$ 228 ([M + H]$^+$). ${}^1H$ NMR (DMSO-$d_6$) selected peaks: $\delta$ 8.00 (d, 1H, $J = 6.2$ Hz), 6.76 (d, 1H, $J = 6.3$ Hz), 4.67 (t, 2H, $J = 5.2$ Hz); ${}^{13}C$ NMR (DMSO-$d_6$) $\delta$ 162.0, 159.6, 157.1, 102.1, 63.3, 47.0, 44.1, 38.3, 26.7, 23.9.

**6-(2-Chloro-pyrimidin-4-yl)-1H-indole (4b).** To a prestirred mixture of 2,4-dichloropyrimidine **1a** (0.83 g, 5.5 mmol), 1H-indol-6-yl boronic acid (0.83 g, 5.0 mmol) in 1,2-dimethoxyethane (40 mL) and saturated aqueous solution of NaHCO$_3$ (4 mL) was added Pd(PPh$_3$)$_4$ (0.30 g, 0.26 mmol). The solution was heated to 85 °C for 6 to 8 h. After the reaction was completed, the solution was cooled down and filtered through Celite. The filtrate was added to ethyl acetate (40 mL) and water (20 mL), and the organic layer was separated, washed with water (3×) and brine (3×), and concentrated. The residue was purified by flash chromatography (silica, EtOAc/hexanes from 1:5 to 1:2) to afford the title compound (0.76 g, yield 66%). $^1$H NMR (CDCl$_3$) $\delta$ 9.74 (s, 1H), 9.23 (d, 1H, $J$ = 1.2 Hz), 8.83 (d, 1H, $J$ = 5.3 Hz), 8.01 (dd, 1H, $J$ = 5.3, 1.2 Hz), 7.60−7.65 (m, 1H), 7.35 (t, 1H, $J$ = 8.2 Hz), 6.94−6.99 (m, 1H). LC-MS (ESI positive mode) $m/z$ 230 ([M + H]$^+$) .

**5-(2-Chloro-pyrimidin-4-yl)-furan-2-carbaldehyde (4c).** To a degassed (nitrogen) solution of 2,4-dichloropyrimidine **1a** (3.8 g, 25.51 mmol) and 5-formyl-2-furan boronic acid (3 g, 21.44 mmol) in 1,2-dimethoxy ethane [DME] (100 mL) were added aq. Na$_2$CO$_3$ (5.5 g in 10 mL of H$_2$O, 51.0 mmol) and Pd(dppf)Cl$_2$·CH$_2$Cl$_2$ [1:1] (0.87 g, 1.07 mmol). The reaction mixture was stirred to 80 °C for 4 h. It was cooled to rt and poured into water and extracted with CH$_2$Cl$_2$ (3 × 40 mL). The combined organic extracts were washed with brine, dried over Na$_2$SO$_4$, and concentrated under reduced pressure to obtain the crude residue. The crude material was purified by column chromatography (EtOAc/Hexane 1:2) to afford **4c** (3.01 g; yield, 67%) as an off-white solid. LC-MS (ESI positive mode) $m/z$ 209 ([M + H]$^+$).

Following a procedure similar to that of **4c**, the following intermediates were synthesized.

**2-Chloro-4-(2-fluoro-pyridin-4-yl)-pyrimidine (4e).** The title compound was synthesized from **1a** and 2-fluoro-4-pyridine boronic acid **3c** (yield, 61%). LC-MS (ESI positive mode) $m/z$ 210 ([M + H]$^+$); $^1$H NMR (CDCl$_3$): $\delta$ 8.85 (d, 1H), 8.47 (d, 1H), 7.87 (dt, 1H), 7.75 (d, 1H), 7.67−7.68 (m, 1H).

**5-(2-Chloro-pyrimidin-4-yl)-pyridine-3-carbaldehyde (4f).** The title compound was synthesized from **1a** and 5-formyl-3-pyridine boronic acid pinacol ester **3a** (yield, 80%). LC-MS (ESI positive mode) $m/z$ 220 ([M + H]$^+$).

**5-(2-Chloro-pyrimidin-4-yl)-thiophene-2-carbaldehyde (4h).** The title compound was synthesized from **1a** and 5-formyl-2-thiophene boronic acid **3e** (yield, 84%). LC-MS (ESI positive mode) $m/z$ 225 ([M + H]$^+$); $^1$H NMR (CDCl$_3$) $\delta$ 10.64 (s, 1H), 8.68 (d, 1H), 7.66 (m, 2H), 7.57 (d, 1H).

**4-(2-Chloro-pyrimidin-4-yl)-thiophene-2-carbaldehyde (4j).** The title compound was synthesized from **1a** and 2-formyl-4-thiophene boronic acid **3f** (yield, 92%). LC-MS (ESI positive mode) $m/z$ 225 ([M + H]$^+$).

**4-(2-Chloro-pyrimidin-4-yl)-furan-2-carbaldehyde (4l).** The title compound was synthesized from **1a** and 2-formyl-4-furan boronic acid **3g** (yield, 61%). LC-MS (ESI positive mode) $m/z$ 209 ([M + H]$^+$).

**5-(2-Chloro-pyrimidin-4-yl)-furan-3-carbaldehyde (4n).** The title compound was synthesized from **1a** and 4-formyl-2-furan boronic acid **3h** (yield, 70%). LC-MS (ESI positive mode) $m/z$ 209 ([M + H]$^+$).

**2-Chloro-4-(2-fluoro-pyridin-4-yl)-5-methyl-pyrimidine (4p).** The title compound was synthesized from 2,4-dichloro-5-methylpyrimidine **1b** and 2-fluoro-4-pyridine boronic acid **3c** (yield, 58%). LC-MS (ESI positive mode) $m/z$ 224 ([M + H]$^+$).

**6-(2-Chloro-5-methyl-pyrimidin-4-yl)-1H-indole (4q).** The title compound was synthesized from 2,4-dichloro-5-methylpyrimidine **1b** and 6-indole boronic acid **3a** (yield, 77%). LC-MS (ESI positive mode) $m/z$ 244 ([M + H]$^+$).

**[5-(2-Chloro-pyrimidin-4-yl)-furan-2-yl]-methanol (4d).** To a solution of **4c** (2.25 g, 10.79 mmol) in THF (40 mL), cooled at 0 °C, was added NaBH$_4$ (0.82 g, 21.58 mmol), followed by MeOH (10 mL) dropwise, maintaining the temperature at 0 °C. The resulting mixture was brought to rt and stirred for 30 min. The reaction mixture was quenched with H$_2$O and extracted with EtOAc (3 × 25 mL). The combined organic extracts were washed with H$_2$O, followed by brine, dried over Na$_2$SO$_4$, and concentrated under reduced pressure to

furnish without purification 2.14 g of compound **4d** (yield, 94%). LC-MS (ESI positive mode) $m/z$ 211 ([M + H]$^+$).

Following a procedure similar to that of **4d**, the following intermediates were synthesized.

**[5-(2-Chloro-pyrimidin-4-yl)-pyridin-3-yl]-methanol (4g).** The title compound was synthesized from **4f** (yield, 75%). LC-MS (ESI positive mode) $m/z$ 222 ([M + H]$^+$).

**[5-(2-Chloro-pyrimidin-4-yl)-thiophen-2-yl]-methanol (4i).** The title compound was synthesized from **4h** (yield, 70%). LC-MS (ESI positive mode) $m/z$ 227 ([M + H]$^+$); $^1$H NMR (CDCl$_3$) $\delta$ 8.62 (d, 1H), 7.55 (m, 2H), 7.25 (d, 1H), 4.83 (s, 2H), 4.68 (bs, 1H).

**[4-(2-Chloro-pyrimidin-4-yl)-thiophen-2-yl]-methanol (4k).** The title compound was synthesized from **4j** (yield, 80%). LC-MS (ESI positive mode) $m/z$ 227 ([M + H]$^+$).

**[4-(2-Chloro-pyrimidin-4-yl)-furan-2-yl]-methanol (4m).** The title compound was synthesized from **4l** (yield, 93%). LC-MS (ESI positive mode) $m/z$ 211 ([M + H]$^+$).

**[5-(2-Chloro-pyrimidin-4-yl)-furan-3-yl]-methanol (4o).** The title compound was synthesized from **4n** (yield, 78%). LC-MS (ESI positive mode) $m/z$ 211 ([M + H]$^+$).

**4-(3-Allyloxymethyl-piperidin-1-yl)-2-chloro-pyrimidine (5a).** A solution of **4a** (1.12 g, 4.91 mmol) in anhydrous THF (40 mL) was added allyl bromide (1.5 mL, 17.3 mmol) and cooled in an acetone/dry ice bath. Sodium hydride (60% in mineral oil, 0.910 g, 22.7 mmol) was added to the mixture under N$_2$, after 10 min, the dry ice bath was removed, and the resulting mixture was stirred at room temp overnight. The reaction was quenched by the addition of dry ice powder and MeOH, and then concentrated under reduced pressure. The residue was diluted with aqueous NaHCO$_3$ and extracted with CH$_2$Cl$_2$ thrice. After workup, the crude product was purified by flash chromatography (silica, 30−60% EtOAc in hexanes) to afford the title compound as a colorless oil (0.68 g; yield, 52%). LC-MS (ESI positive mode) $m/z$ 268/270 ([M + H]$^+$); $^1$H NMR (CDCl$_3$) $\delta$ 7.89 (d, 1H, $J$ = 6.2 Hz), 6.35 (d, 1H, $J$ = 6.2 Hz), 5.82 (ddt, 1H, $J$ = 17.2, 10.4, 5.6 Hz), 5.20 (ddt, 1H, $J$ = 17.2, 1.7, 1.7 Hz), 5.10 (ddt, 1H, $J$ = 10.4, 1.6, 1.5 Hz), 4.08 (b s, 2H), 3.88 (dm, 2H, $J$ = 7.1 Hz), 3.29 (dd, 1H, $J$ = 9.4, 5.0 Hz), 3.22 (dd, 1H, $J$ = 9.3, 7.7 Hz), 3.05 (ddd, 1H, $J$ = 13.1, 10.6, 3.0 Hz), 2.86 (dd, 1H, $J$ = 13.0, 9.7 Hz), 1.86−1.74 (m, 2H), 1.72−1.64 (m, 1H), 1.51−1.39 (m, 1H), 1.36−1.13 (m, 1H); $^{13}$C NMR (CDCl$_3$) $\delta$ 162.4, 160.6, 156.9, 134.7, 116.9, 101.3, 72.1, 72.0, 47.8, 44.8, 36.2, 27.3, 24.1.

**1-Allyl-6-(2-chloro-pyrimidin-4-yl)-1H-indole (5c).** A solution of **4b** (115 mg, 0.5 mmol) and NaH (73 mg, 60% in mineral oil, 0.9 mmol) in 2 mL of dried DMF was stirred at room temperature for 30 min. Allyl bromide (121 mg, 1.0 mmol) in 1 mL of dried DMF was added to the solution. The mixture was stirred at room temperature overnight. The reaction was quenched by adding water slowly. The mixture was extracted with EtOAc thrice, and the combined extracts were washed with water 3 times and then washed with brine once. The product **5c** (112 mg; yield, 83%) was obtained by flash column chromatography. (EtOAc/hexanes from 1:10 to 1:4) LC-MS (ESI positive mode) $m/z$ 270 ([M + H]$^+$); $^1$H NMR (CDCl$_3$) $\delta$ 8.54 (d, 1H), 8.21 (s, 1H), 7.75 (d, 1H), 7.71 (d, 1H), 7.66 (d, 1H), 7.25 (d, 1H), 6.56 (d, 1H), 6.02 (m, 1H), 5.25 (d, 1H), 5.12 (d, 1H), 4.83 (d, 2H).

Following a procedure similar to that of **5c**, the following intermediates were synthesized.

**1-But-3-enyl-6-(2-chloro-pyrimidin-4-yl)-1H-indole (5b).** The title compound was synthesized from **4b** and 4-bromo-1-butene (yield, 62%). LC-MS (ESI positive mode) $m/z$ 284 ([M + H]$^+$).

**1-Allyl-6-(2-chloro-5-methyl-pyrimidin-4-yl)-1H-indole (5j).** The title compound was synthesized from **4q** and allyl bromide (yield, 77%). LC-MS (ESI positive mode) $m/z$ 284 ([M + H]$^+$).

**4-(5-Allyloxymethyl-furan-2-yl)-2-chloro-pyrimidine (5d).** A mixture of **4d** (10 g, 47.5 mmol), KOH (5.3 g, 94.6 mmol), and tetrabutyl ammonium hydrogen sulfate [TBAHSO$_4$] (0.79 g, 2.38 mmol) in allyl bromide (40 mL, 4 vol) was stirred at rt for 12 h. The reaction mixture was quenched with water and extracted with CH$_2$Cl$_2$ (3 × 20 mL). The combined organic extracts were washed with water, brine, dried (Na$_2$SO$_4$), and concentrated under reduced pressure to obtain the crude residue, which was purified by column chromatography (using

15% EtOAc/hexanes) to furnish **5d** (10.0 g; yield, 84%) as a pale yellow oil. LC-MS (ESI positive mode) $m/z$ 251 ([M + H]$^+$).

Following a procedure similar to that of **5d**, the following intermediates were synthesized.

*4-(5-Allyloxymethyl-pyridin-3-yl)-2-chloro-pyrimidine (5e).* The title compound was synthesized from **4g** and allyl bromide (yield, 46%). LC-MS (ESI positive mode) $m/z$ 262 ([M + H]$^+$).

*4-(5-Allyloxymethyl-thiophen-2-yl)-2-chloro-pyrimidine (5f).* The title compound was synthesized from **4i** and allyl bromide (yield, 80%). LC-MS (ESI positive mode) $m/z$ 267 ([M + H]$^+$).

*4-(5-Allyloxymethyl-thiophen-3-yl)-2-chloro-pyrimidine (5g).* The title compound was synthesized from **4k** and allyl bromide (yield, 80%). LC-MS (ESI positive mode) $m/z$ 267 ([M + H]$^+$).

*4-(5-Allyloxymethyl-furan-3-yl)-2-chloro-pyrimidine (5h).* The title compound was synthesized from **4m** and allyl bromide (yield, 82%). LC-MS (ESI positive mode) $m/z$ 251 ([M + H]$^+$).

*4-(4-Allyloxymethyl-furan-2-yl)-2-chloro-pyrimidine (5i).* The title compound was synthesized from **4o** and allyl bromide (yield, 74%). LC-MS (ESI positive mode) $m/z$ 251 ([M + H]$^+$).

*1-Allyloxymethyl-3-nitro-benzene (9a).* The title compound was synthesized from 3-nitrobenzyl alcohol **7a** and allyl bromide (yield, 78%). LC-MS (ESI positive mode) $m/z$ 194 ([M + H]$^+$); $^1$H NMR (CDCl$_3$): $\delta$ 8.27 (s, 1H), 8.18 (dd, 1H), 7.73 (dd, 1H), 7.57 (t, 1H), 6.01 (m, 1H), 5.38 (m, 1H), 5.29 (m, 1H), 4.65 (s, 2H), 4.13 (dt, 2H).

*4-(3-Allyloxymethyl phenyl)-2-chloro pyrimidine (9b).* The title compound was synthesized from **7b** and allyl bromide (yield, 55%). LC-MS (ESI positive mode) $m/z$ 261 ([M + H]$^+$); $^1$H NMR (CDCl$_3$) $\delta$ 8.62 (d, 1H), 8.06 (br, 1H), 8.00 (dt, 1H), 7.66 (d, 1H), 7.54−7.46 (m, 2H), 6.02 − 5.93 (m, 1H), 5.27 (ddq, 2H), 4.60 (s, 2H), 4.08 (dq, 2H); $^{13}$C NMR (CDCl$_3$) $\delta$ 167.1, 161.9, 159.9, 139.7, 135.3, 134.6, 131.2, 129.7, 129.3, 126.6, 117.5, 115.4, 71.7, 71.6. Anal. Calcd. for C$_{12}$H$_{14}$ClNO4: C, 53.05; H, 5.19; N, 5.16; Cl: 13.05. Found: C, 53.09; H, 5.30; N, 5.14; Cl, 13.37. IR (KBr pellet): 1568, 1535, 1344, 1186, 1079 cm$^{-1}$.

*2-(2-Methoxy−ethoxy)-5-nitro-benzaldehyde (6c).* To a mixture of 2-hydroxy-5-nitrobenzaldehyde **6b** (5 g, 29.9 mmol) and 1-bromo-2-methoxyethane (5.6 mL, 59.8 mmol) in DMF (50 mL, 10 vol)) was added K$_2$CO$_3$ (6.25 g, 45.0 mmol), and the resulting mixture was stirred at 100−105 °C for 6 h. The reaction mixture was cooled to 0 °C and quenched with water. The product was extracted with CH$_2$Cl$_2$ thrice, and the combined organic extracts were dried over Na$_2$SO$_4$ and concentrated under reduced pressure to furnish an oil, which was purified by column chromatography (EtOAc/Hexane) to obtain 5.8 g of **6c** (yield, 86%). LC-MS (ESI positive mode) $m/z$ 226 ([M + H]$^+$).

*2-(2-Chloro ethoxy)-5-nitro-benzaldehyde (6d) and [2-(2-Chloro-ethoxy)-5-nitro-phenyl]-methanol (7b).* The title compounds were synthesized according to a literature procedure.[22]

*Allyl Methyl-(3 nitro benzyl) Amine (8a).* To a solution of 3-nitrobenzaldehyde **6a** (20 g, 132.4 mmol) in CH$_2$Cl$_2$ (500 mL) was added N-allyl methyl amine (18.8 mL, 198.6 mmol), and the resulting mixture was stirred at rt for 12 h, after which Na(OAc)$_3$BH (56.13 g, 265 mmol) was added portion wise and stirred for additional 4 h. The reaction mixture was then quenched with sat. NH$_4$Cl solution and extracted with CH$_2$Cl$_2$ (3 × 150 mL). The combined organic extracts were dried over Na$_2$SO$_4$ and concentrated under reduced pressure to give the crude material, which was purified by column chromatography (EtOAc/hexane 1:19) to afford **8a** (25.9 g; yield, 95%) as a pale yellow syrup. LC-MS (ESI positive mode) $m/z$ 207 ([M + H]$^+$); $^1$H NMR (CDCl$_3$) $\delta$ 8.20 (s, 1H), 8.11 (dd, 1H), 7.68 (dd, 1H), 7.48 (t, 1H), 5.85−5.94 (m, 1H), 5.20 (t, 1H), 3.60 (s, 2H), 3.07 (dd, 1H), 2.22 (s, 3H); $^{13}$C NMR (CDCl$_3$) $\delta$ 148.4, 141.5, 135.20, 134.9, 129.1, 123.7, 122.1, 118.1, 60.52, 60.50. Anal. Calcd. for C$_{11}$H$_{14}$N$_2$O$_2$: C, 64.06; H, 6.84; N, 13.58. Found: C, 62.31; H, 6.69; N, 13.25. IR (KBr pellet): 2787, 1528, 1349, 924, 733 cm$^{-1}$.

Following a procedure similar to that of **8a**, the following intermediates were synthesized:

*Allyl-[2-(2-methoxy−ethoxy)-5-nitro-benzyl]-methyl-amine (8b).* The title compound was synthesized from **6c** and N-allyl methyl amine (yield, 92%). LC-MS (ESI positive mode) $m/z$ 281 ([M + H]$^+$).

*Allyl-[2-(2-chloro-ethoxy)-5-nitro-benzyl]-methyl-amine (8c).* The title compound was synthesized from **6d** and N-allyl methyl amine (yield, 85%). LC-MS (ESI positive mode) $m/z$ 285 ([M + H]$^+$).

*[5-(2-Chloro-pyrimidin-4-yl)-furan-3-yl]-methanol (8d).* To a solution of **8c** (2 g, 7.02 mmol) in N,N-dimethylacetamide (DMA, 10 mL) was added pyrrolidine (4 mL, 2 vol), and the resulting mixture was stirred at 90 °C for 20 h. The reaction mixture was brought to rt and quenched with water (20 mL) and extracted in ethyl acetate (3 × 20 mL). The combined organic extracts were washed with water, brine, dried (Na$_2$SO$_4$), and concentrated under reduced pressure to afford the crude **8d** (1.68 g; yield, 75%) as thick syrup. This intermediate was taken forward for the next step without any purification. LC-MS (ESI positive mode) $m/z$ 320 ([M + H]$^+$).

*1-[2-(2-Allyloxymethyl-4-nitro phenoxy] pyrrolidine (9c).* Following a procedure similar to that of **8d**, the title compound was synthesized from **9b** and pyrrolidine (yield, 78%). LC-MS (ESI positive mode) $m/z$ 307 ([M + H]$^+$). Theoretical HRMS ([M + H]$^+$) 307.1652, found 307.1653; $^1$H NMR (CDCl$_3$) $\delta$ 8.33 (d, 1H), 8.17 (dd, 1H), 6.91 (d, 1H), 6.03−5.93 (m, 1H), 5.37−5.23 (m, 2H), 4.56 (s, 2H), 4.26 (t, 2H), 4.12 (dt, 2H), 2.99 (t, 2H), 2.71−2.68 (m, 4H), 1.90−1.86 (m, 4H); $^{13}$C NMR (CDCl$_3$) $\delta$ 23.8, 54.7, 55.1, 66.3, 68.5, 72.2, 110.7, 117.6, 124.3, 125.0, 128.6, 134.6, 141.7, 161.0.

*3-[(Allylmethylamino) methyl] Phenyl Amine (10a).* To a solution of **8a** (6.9 g, 33.5 mmol) in CH$_2$Cl$_2$/MeOH (1:1, 100 mL), cooled to 0 °C, SnCl$_2$·2H$_2$O (25.4 g, 134 mmol) was added. The reaction mixture was gradually raised to rt and stirred for 12 h. After completion of the reaction, the solvent from the reaction mixture was removed under reduced pressure, and the residue was taken into aqueous Na$_2$CO$_3$ and CH$_2$Cl$_2$ (100 mL). The reaction mixture was filtered through filter paper. The organic layer was separated out from the filtrate, and the aqueous layer was extracted with CH$_2$Cl$_2$ (3 × 50 mL). The combined organic extracts were dried (Na$_2$SO$_4$) and concentrated under reduced pressure to afford 7 (5.8 g; yield, 98%) as a thick syrup, which was used for the next step without further purification. LC-MS (ESI positive mode) $m/z$ 177 ([M + H]$^+$). $^1$H NMR (CDCl$_3$) $\delta$ 7.09 (t, 1H), 6.57−6.69 (m, 2H), 6.55 (dd, 1H), 5.85−5.95 (m, 1H), 5.12−5.17 (m, 2H), 3.67 (br, 1H), 3.39 (s, 2H), 3.02 (d, 2H), 2.18 (s, 3H); $^{13}$C NMR (CDCl$_3$) $\delta$ 146.4, 140.3, 136.0, 129.1, 119.4, 117.4, 115.7, 113.8, 61.7, 60.6, 42.2. Anal. Calcd. for C$_{11}$H$_{16}$N$_2$: C, 74.96; H, 9.15; N, 15.89. Found: 74.34; H, 9.04; N, 15.68. IR (KBr pellet): 3346, 3210, 2782, 1605, 1460, 1294, 921, 785, 696 cm$^{-1}$.

Following a procedure similar to that of **10a**, the following intermediates were synthesized.

*3-[(Allyl-methyl-amino)-methyl]-4-(2-methoxy−ethoxy)-phenyl-amine (10b).* The title compound was synthesized from **8b** (yield, 64%). LC-MS (ESI positive mode) $m/z$ 251 ([M + H]$^+$).

*3-[(Allyl-methyl-amino)-methyl]-4-(2-pyrrolidin-1-yl-ethoxy)-phenylamine (10c).* The title compound was synthesized from **8d** (yield, 88%). LC-MS (ESI positive mode) $m/z$ 290 ([M + H]$^+$).

*3-Allyloxymethyl-phenylamine (10d).* The title compound was synthesized from **9a** (yield, 91%). LC-MS (ESI positive mode) $m/z$ 164 ([M + H]$^+$).

*3-Allyloxymethyl-4-(2-pyrrolidin-1-yl-ethoxy)phenylamine (10e).* The title compound was synthesized from **9c** (yield, 89%). LC-MS (ESI positive mode) $m/z$ 277 ([M + H]$^+$). Theoretical HRMS [M + H]$^+$ 277.1911, found 277.1916; $^1$H NMR (MeOD-$d_4$) $\delta$ 6.82−6.78 (m, 2H), 6.69 (dd, 1H), 5.93−5.83 (m, 1H), 5.26−5.11 (m, 2H), 4.45 (s, 2H), 4.20 (t, 2H), 3.97 (dt, 2H), 3.56 (t, 2H); $^{13}$C NMR (MeOD-$d_4$) $\delta$ 149.4, 140.2, 134.7, 127.6, 118.2, 116.5, 116.2, 113.9, 70.8, 67.3, 64.6, 54.5, 54.1, 22.6; IR (KBr pellet): 1626, 1502, 1225, 1084, 798 cm$^{-1}$.

*{3-[(Allyl-methyl-amino)-methyl]-phenyl}-[4-(5-allyloxymethyl-furan-2-yl)-pyrimidin-2-yl]-amine (11c).* To a solution of **5d** (80 mg, 0.319 mmol) and **10a** (60 mg, 0.340 mmol) in n-butanol (2 mL) was added 4 M HCl (0.2 mL), and the resulting mixture was heated to 80−100 °C for 12 h. The reaction mixture was brought to rt, and the solvent was removed under reduced pressure. The residue was dissolved in minimum amount of MeOH and purified by preparative

rpHPLC to furnish **11c** as a TFA salt (112 mg; yield, 90%). LC-MS (ESI positive mode) *m/z* 391 ([M + H]$^+$).

Following a procedure similar to that of **11c**, the following intermediates were synthesized.

*{3-[(Allyl-methyl-amino)-methyl]-phenyl}-[4-(3-allyloxymethyl-piperidin-1-yl)-pyrimidin-2-yl]-amine (11a).* The title compound was synthesized from **5a** and **10a** and was obtained as a crude yellow residue (HPLC purity = 94% at 254 nm), which was used for the next step of the reaction without further purification. LC-MS (ESI positive mode) *m/z* 408 ([M + H]$^+$).

*{3-[(Allyl-methyl-amino)-methyl]-phenyl}-[4-(1-but-3-enyl-1H-indol-6-yl)-pyrimidin-2-yl]-amine (11b).* The title compound was synthesized from **5b** and **10a** (yield, 94%). LC-MS (ESI positive mode) *m/z* 424 ([M + H]$^+$).

*{3-[(Allyl-methyl-amino)-methyl]-phenyl}-[4-(2-fluoro-pyridin-4-yl)-pyrimidin-2-yl]-amine (11d).* The title compound was synthesized from **4e** and **10a** (yield, 86%). LC-MS (ESI positive mode) *m/z* 350 ([M + H]$^+$).

*{3-[(Allyl-methyl-amino)-methyl]-phenyl}-[4-(5-allyloxymethyl-pyridin-3-yl)-pyrimidin-2-yl]-amine (11f).* The title compound was synthesized from **5e** and **10a** (yield, 84%). LC-MS (ESI positive mode) *m/z* 402 ([M + H]$^+$).

*[4-(5-Allyloxymethyl-furan-2-yl)-pyrimidin-2-yl]-(3-allyloxymethyl-phenyl)-amine (11g).* The title compound was synthesized from **5d** and **10d** (yield, 93%). LC-MS (ESI positive mode) *m/z* 478 ([M + H]$^+$).

*[4-(1-Allyl-1H-indol-6-yl)-pyrimidin-2-yl]-(3-allyloxymethyl-phenyl)-amine (11h).* The title compound was synthesized from **5c** and **10d** (yield, 79%). LC-MS (ESI positive mode) *m/z* 397 ([M + H]$^+$).

*(3-Allyloxymethyl-phenyl)-[4-(5-allyloxymethyl-pyridin-3-yl)-pyrimidin-2-yl]-amine (11i).* The title compound was synthesized from **5e** and **10d** (yield, 92%). LC-MS (ESI positive mode) *m/z* 389 ([M + H]$^+$).

*[3-[(Allyl-methyl-amino)-methyl]-4-(2-pyrrolidin-1-yl-ethoxy)-phenyl]-[4-(5-allyloxymethyl-furan-2-yl)-pyrimidin-2-yl]-amine (12a).* The title compound was synthesized from **5d** and **10c** (yield, 72%). LC-MS (ESI positive mode) *m/z* 504 ([M + H]$^+$).

*[3-[(Allyl-methyl-amino)-methyl]-4-(2-pyrrolidin-1-yl-ethoxy)-phenyl]-[4-(5-allyloxymethyl-thiophen-2-yl)-pyrimidin-2-yl]-amine (12b).* The title compound was synthesized from **5f** and **10c** (yield, 62%). LC-MS (ESI positive mode) *m/z* 520 ([M + H]$^+$).

*[3-[(Allyl-methyl-amino)-methyl]-4-(2-methoxy−ethoxy)-phenyl]-[4-(5-allyloxymethyl-thiophen-2-yl)-pyrimidin-2-yl]-amine (12c).* The title compound was synthesized from **5f** and **10b** (yield, 72%). LC-MS (ESI positive mode) *m/z* 481 ([M + H]$^+$).

*[3-[(Allyl-methyl-amino)-methyl]-4-(2-methoxy−ethoxy)-phenyl]-[4-(5-allyloxymethyl-furan-2-yl)-pyrimidin-2-yl]-amine (12d).* The title compound was synthesized from **5d** and **10b** (yield, 68%). LC-MS (ESI positive mode) *m/z* 465 ([M + H]$^+$).

*[4-(1-Allyl-1H-indol-6-yl)-pyrimidin-2-yl]-[3-allyloxymethyl-4-(2-pyrrolidin-1-yl-ethoxy)-phenyl]-amine (12e).* The title compound was synthesized from **5c** and **10e** (yield, 71%). LC-MS (ESI positive mode) *m/z* 510 ([M + H]$^+$); $^1$H NMR (MeOD-$d_4$) δ 8.20 (s, 1H), 8.15 (d, 1H), 7.81 (d, 1H), 7.64 (d, 1H), 7.43 (d, 1H), 7.33 (m, 1H), 7.02 (d, 1H), 6.43 (d, 1H), 5.85 (m, 2H), 5.15 (d, 1H), 5.06 (m, 2H), 4.95 (d, 1H), 4.79 (m, 2H), 4.55 (s, 2H), 4.30 (m, 2H), 4.08 (m, 2H), 3.68 (m, 2H), 3.60 (m, 2H), 3.18 (m, 2H), 2.10 (m, 2H), 1.91 (m, 2H).

*[3-Allyloxymethyl-4-(2-pyrrolidin-1-yl-ethoxy)-phenyl]-[4-(5-allyloxymethyl-thiophen-2-yl)-pyrimidin-2-yl]-amine (12f).* The title compound was synthesized from **5f** and **10e** (yield, 87%). LC-MS (ESI positive mode) *m/z* 507 ([M + H]$^+$).

*[3-Allyloxymethyl-4-(2-pyrrolidin-1-yl-ethoxy)-phenyl]-[4-(5-allyloxymethyl-thiophen-3-yl)-pyrimidin-2-yl]-amine (12g).* The title compound was synthesized from **5g** and **10e** (yield, 88%). LC-MS (ESI positive mode) *m/z* 507 ([M + H]$^+$).

*[4-(5-Allyloxymethyl-furan-3-yl)-pyrimidin-2-yl]-[3-allyloxymethyl-4-(2-pyrrolidin-1-yl-ethoxy)-phenyl]-amine (12h).* The title compound was synthesized from **5h** and **10e** (yield, 92%). LC-MS (ESI positive mode) *m/z* 491 ([M + H]$^+$).

*[4-(5-Allyloxymethyl-furan-2-yl)-pyrimidin-2-yl]-[3-allyloxymethyl-4-(2-pyrrolidin-1-yl-ethoxy)-phenyl]-amine (12i).* The title compound

was synthesized from **5d** and **10e** (yield, 96%). LC-MS (ESI positive mode) *m/z* 491 ([M + H]$^+$).

*[4-(4-Allyloxymethyl-furan-2-yl)-pyrimidin-2-yl]-[3-allyloxymethyl-4-(2-pyrrolidin-1-yl-ethoxy)-phenyl]-amine (12j).* The title compound was synthesized from **5i** and **10e** (yield, 63%). LC-MS (ESI positive mode) *m/z* 491 ([M + H]$^+$).

*[4-(5-Allyloxymethyl-pyridin-3-yl)-pyrimidin-2-yl]-[3-allyloxymethyl-4-(2-pyrrolidin-1-yl-ethoxy)-phenyl]-amine (12k).* The title compound was synthesized from **5e** and **10e** (yield, 68%). LC-MS (ESI positive mode) *m/z* 502 ([M + H]$^+$).

*[3-Allyloxymethyl-4-(2-pyrrolidin-1-yl-ethoxy)-phenyl]-[4-(2-fluoro-pyridin-4-yl)-pyrimidin-2-yl]-amine (12l).* The title compound was synthesized from **4e** and **10e** (yield, 81%). LC-MS (ESI positive mode) *m/z* 450 ([M + H]$^+$); $^1$H NMR (CDCl$_3$) δ 8.47−8.35 (m, 3H), 7.81 (d, 1H), 7.62 (dd, 1H), 7.50 (dd, 1H), 7.39 (s, 1H), 6.93 (d, 1H), 5.90−6.00 (dq, 1H), 5.33 (dd, 1H), 5.17 (dd, 1H), 4.58 (s, 2H), 4.45 (s, 2H), 4.10 (d, 2H), 4.04 (s, 2H), 3.65 (br s, 2H), 3.10 (m, 2H), 2.21−2.10 (m, 4H).

*[3-Allyloxymethyl-4-(2-pyrrolidin-1-yl-ethoxy)-phenyl]-[4-(2-fluoro-pyridin-4-yl)-5-methyl-pyrimidin-2-yl]-amine; compound with methane (12n).* The title compound was synthesized from **4p** and **10e** (yield, 83%). LC-MS (ESI positive mode) *m/z* 479 ([M + H]$^+$).

*[4-(1-Allyl-1H-indol-6-yl)-5-methyl-pyrimidin-2-yl]-[3-allyloxymethyl-4-(2-pyrrolidin-1-yl-ethoxy)-phenyl]-amine (12p).* The title compound was synthesized from **5c** and **10e** (yield, 86%). LC-MS (ESI positive mode) *m/z* 524 ([M + H]$^+$).

*{3-[(Allyl-methyl-amino)-methyl]-phenyl}-[4-(2-but-3-enyloxy-pyridin-4-yl)-pyrimidin-2-yl]-amine (11d).* To a solution of 3-buten-1-ol (30 μL, 0.349 mmol), in anhydrous THF (2 mL), was added 60% sodium hydride in mineral oil (16 mg, 0.400 mmol) at 0 °C. The solution was stirred at 0 °C was 0.5 h and then slowly allowed to warm to rt. To this solution of sodium salt of 3-buten-1-ol was added a solution of **11c** (TFA salt, 120 mg, 0.269 mmol) in anhydrous THF (2 mL). The resulting mixture was heated at 70 °C for 12 h, quenched with water, and extracted with CH$_2$Cl$_2$. The combined organic layers were dried over Na$_2$SO$_4$. Evaporation and purification by preparative HPLC afforded the title compound in 40% yield. LC-MS (ESI positive mode) *m/z* 402 ([M + H]$^+$).

Following a procedure similar to that of **11d**, the following intermediates were synthesized.

*[3-Allyloxymethyl-4-(2-pyrrolidin-1-yl-ethoxy)-phenyl]-[4-(2-but-3-enyloxy-pyridin-4-yl)-pyrimidin-2-yl]-amine (12m).* The title compound was synthesized from **12l** and 3-buten-1-ol (yield, 48%). LC-MS (ESI positive mode) *m/z* 502([M + H]$^+$).

*[3-Allyloxymethyl-4-(2-pyrrolidin-1-yl-ethoxy)-phenyl]-[4-(2-but-3-enyloxy-pyridin-4-yl)-5-methyl-pyrimidin-2-yl]-amine (12o).* The title compound was synthesized from **12n** and 3-buten-1-ol (yield, 36%). LC-MS (ESI positive mode) *m/z* 516 ([M + H]$^+$).

*15-(2-Methoxyethoxy)-12-methyl-7-oxa-25-thia-12,19,21,24-tetraaza-tetracyclo[18.3.1.1(2,5).1(14,18)]hexacosa-1(24),2,4,9,14-(26),15,17,20,22-nonaene (14i).* To **12i** (TFA salt, 100 mg, 0.170 mmol) in CH$_2$Cl$_2$ (50 mL) at ambient temperature was added 4 M HCl until the pH reached 2.0−2.2. The solution was degassed (N$_2$), and Grubbs second generation catalyst (14 mg, 0.017 mmol) was added in two portions (7 mg each) at 1 h intervals. The resulting mixture was stirred at 40−45 °C for 4 h. The reaction mixture was cooled and concentrated under reduced pressure to furnish an oil, which was purified by preparative rpHPLC to obtain 63 mg of **14i** as a TFA salt (yield, 66%; >95% trans by $^1$H NMR). LC-MS (ESI positive mode) *m/z* 463 ([M + H]$^+$); $^1$H NMR (MeOD-$d_4$): δ 8.56 (d, 1H), 8.38 (d, 1H), 8.29 (br s, 1H), 7.17 (d, 1H), 7.11−7.06 (m, 2H), 7.03−7.01 (m, 1H), 5.99 (dt, 1H), 5.84 (dt, 1H), 4.66 (s, 2H$_2$), 4.57 (s, 2H), 4.37 (t, 2H), 4.18 (d, 2H), 4.09 (d, 2H), 3.79 (br s, 2H), 3.69 (t, 2H), 3.35−3.34 (m, 2H), 2.21−2.07 (m, 4H).

Following a procedure similar to that of **14i**, the following compounds were synthesized.

*14-Methyl-19-oxa-1,5,7,14,26-pentaaza-tetracyclo[19.3.1.1-(2,6).1(8,12)]heptacosa-2(26),3,5,8(27), 9,11,16-heptaene (13a).* The title compound was synthesized from **11a** and isolated as freebase (33 mg, 15% from **5a** in two steps; mixture of cis/trans 1:9 by $^1$H NMR). LC-MS (ESI positive mode) *m/z* 380 ([M + H]$^+$). For the

major trans isomer: ^{1}H NMR (CDCl$_3$) $\delta$ 8.33 (t, 1H, $J$ = 1.6 Hz), 7.92 (d, 1H, $J$ = 6.1), 7.57 (b s, 1H), 7.16 (t, 1H, $J$ = 7.7 Hz), 6.85 (d, 1H, $J$ = 7.5 Hz), 6.75 (dd, 1H, $J$ = 7.9, 1.3 Hz), 5.98 (d, 1H, $J$ = 6.2 Hz), 5.92 (dm, 1H, $J$ = 15.6 Hz), 5.61 (ddd, 1H, $J$ = 15.7, 4.5, 3.7 Hz), 4.88 (dm, 1H, $J$ = 13.0 Hz), 4.14 (dd, 1H, $J$ = 15.1, 1.3 Hz), 3.91 (dd, 1H, $J$ = 14.9, 4.6 Hz), 3.80 (d, 1H, $J$ = 13.3 Hz), 3.58 (d, 1H, $J$ = 12.4 Hz), 3.47 (m, 2H), 3.22 (d, 1H, $J$ = 12.4 Hz), 3.20 (t, 1H, $J$ = 5.4 Hz), 3.05 (dd, 1H, $J$ = 13.1, 7.4 Hz), 2.93 (m, 1H), 2.87 (m, 1H), 2.16 (s, 3H), 1.95 (m, 1H), 1.83−1.75 (m, 2H), 1.65−1.49 (m, 2H); ^{13}C NMR (CDCl$_3$) $\delta$ 161.9, 159.6, 156.5, 140.6, 140.1, 129.9, 129.3, 128.1, 122.9, 119.6, 117.9, 94.2, 71.2, 68.5, 60.43, 60.38, 46.7, 45.4, 42.9, 36.1, 27.9, 25.2.

*20,22-Etheno-14-methyl-5,7,14,20,26-pentaaza-tetracyclo-[19.3.1.1(2,6).1(8,12)]heptacosa-1(25),2(26),3,5,8(27),9,11,16,21,23-decaene (13b).* The title compound was synthesized from **11b** (yield, 69%; mixture of cis/trans 13:87 by ^{1}H NMR). LC-MS (ESI positive mode) $m/z$ 396 ([M + H]$^+$); ^{1}H NMR (MeOD-$d_4$) $\delta$ 8.27 (m, 1H), 8.10−8.16 (m, 2H), 7.53−7.59 (m, 2H), 7.25−7.40 (m, 3H), 7.03 (m, 2H), 6.42 (m, 1H), 5.50−5.80 (m, 2H), 5.05 (m, 1H), 4.80 (m, 1H), 4.59 (m, 1H), 4.42 (m, 1H), 4.15 (m, 1H), 3.95 (m, 1H).

*19,21-Etheno-14-oxa-5,7,19,25-tetraaza-tetracyclo[18.3.1.1-(2,6).1(8,12)]hexacosa-1(24),2(25),3,5,8(26),9,11,16,20,22-decaene (13c).* The title compound was synthesized from **11c** (yield, 76%; >95% trans by ^{1}H NMR). LC-MS (ESI positive mode) $m/z$ 363 ([M + H]$^+$); ^{1}H NMR (MeOD-$d_4$) $\delta$ 9.04−9.03 (m, 1H), 8.42 (d, 1H) 7.33 (d, 1H) 7.23−7.15 (m, 4H), 6.69 (d, 1H), 6.28 (dt, 1H), 6.20−6.09 (m, 1H), 4.66 (s, 2H), 4.52−4.47 (m, 1H), 4.20 (br d, 2H), 4.11−4.04 (m, 1H), 3.92−3.81 (m, 2H), 2.90−2.84 (m, 3H).

*14-Methyl-20-oxa-5,7,14,22,26-pentaaza-tetracyclo[19.3.1.1-(2,6).1(8,12)]heptacosa-1(25),2(26),3,5,8(27),9,11,16,21,23-decaene (13d).* The title compound was synthesized from **11e** (yield, 52%; >95% trans by ^{1}H NMR). LC-MS (ESI positive mode) $m/z$ 374 ([M + H]$^+$); ^{1}H NMR (MeOD-$d_4$) $\delta$ 9.08 (m, 1H), 8.64 (d, 1H), 8.31 (m, 1H), 7.84 (m, 1H), 7.53−7.52 (dd, 1H), 7.48−7.43 (m, 2H), 7.29−7.27 (m, 1H), 7.18 (m,1H), 6.29−6.21 (m, 1H), 5.90−5.82 (m, 1H), 4.39−3.72 (m, 6H), 2.68 (s, 5H).

*14-Methyl-19-oxa-5,7,14,23,26-pentaaza-tetracyclo[19.3.1.1-(2,6).1(8,12)]heptacosa-1(25),2(26),3,5,8(27),9,11,16,21,23-decaene (13e).* The title compound was synthesized from **11f** (yield, 44%; >95% trans by ^{1}H NMR). LC-MS (ESI positive mode) $m/z$ 374 ([M + H]$^+$); ^{1}H NMR (DMSO-$d_6$) $\delta$ 10.04 (s, 1H), 9.30 (s, 1H), 8.78 (s, 1H), 8.72 (s, 1H), 8.67 (d, 1H), 8.61 (s, 1H), 7.67 (d, 1H), 7.39 (t, 1H), 7.31 (d, 1H), 7.15 (d, 1H), 6.24−6.18 (m, 1H), 5.96−5.88 (m, 1H), 4.75−4.62 (m, 2H), 4.50 (d, 1H), 4.15 (d, 2H), 4.05−3.93 (m, 2H), 3.84−3.76 (m, 1H), 2.68 (s, 1H).

*14,19-Dioxa-5,7,23,26-tetraaza-tetracyclo[19.3.1.1(2,6).1(8,12)]-heptacosa-1(25),2(26),3,5,8(27),9,11,16,21,23-decaene (13f).* The title compound was synthesized from **11g** (yield, 73%; >95% trans by ^{1}H NMR). LC-MS (ESI positive mode) $m/z$ 350 ([M + H]$^+$); ^{1}H NMR (CDCl$_3$) $\delta$ 10.91(s, 1H), 8.67−8.66 (m, 1H), 8.17−8.14 (m, 1H), 7.37−7.32 (m, 1H), 7.28−7.27 (m, 1H), 7.18−7.16 (m, 2H), 6.97 (d, 1H), 6.65 (d, 1H), 6.00 (dt, 1H), 5.89 (dt, 1H), 4.61 (s, 2H), 4.58 (s, 2H), 4.15 (d, 2H), 4.08 (d, 2H).

*12-Methyl-7,25-dioxa-12,19,21,24-tetraaza-tetracyclo[18.3.1.1-(2,5).1(14,18)]hexacosa-1(24),2,4,9,14(26),15,17,20,22-nonaene (13g).* The title compound was synthesized from **11h** (yield, 51%; mixture of cis/trans 15:85 by ^{1}H NMR). LC-MS (ESI positive mode) $m/z$ 369 ([M + H]$^+$); ^{1}H NMR (MeOD-$d_4$) $\delta$ 8.68 (m, 1H), 8.37 (m, 1H), 8.40 (m, 1H), 8.21 (m, 1H), 7.71 (m, 2H), 7.48 (m, 2H), 7.30 (m, 2H), 6.62 (m, 1H), 5.75 (m, 2H), 4.46 (m, 2H), 4.25 (m, 2H), 3.75−3.95 (m, 2H), 2.87 (s, 3H), 2.75 (m, 2H).

*7,12,25-trioxa-19,21,24-triaza-tetracyclo[18.3.1.1(2,5).1(14,18)]-hexacosa-1(24),2,4,9,14(26),15,17,20,22-nonaene (13h).* The title compound was synthesized from **11i** (yield, 46%; >95% trans by ^{1}H NMR). LC-MS (ESI positive mode) $m/z$ 361 ([M + H]$^+$); ^{1}H NMR (DMSO-$d_6$) $\delta$ 9.29 (s, 1H), 8.78 (s, 1H), 8.63 (d, 1H), 8.57 (s, 1H), 8.52 (s, 1H), 7.62 (d, 1H), 7.28 (t, 1H), 7.14 (d, 1H), 6.98 (d, 1H), 5.90−5.81 (m, 2H), 4.62 (s, 2H), 4.49 (s, 2H), 4.09−4.05 (m, 4H).

*19,21-Etheno-11-(2-(pyrrolidin-1-yl)ethoxy)-14-oxa-5,7,19,25-tet-raaza-tetracyclo[18.3.1.1(2,6).1(8,12)]hexacosa-1(24),2(25),3,5,8-(26),9,11,16,20,22-decaene (14a).* The title compound was synthesized from **12a** (yield, 65%; >95% trans by ^{1}H NMR). LC-MS (ESI positive mode) $m/z$ 476 ([M + H]$^+$); ^{1}H NMR (MeOD-$d_4$) $\delta$ 9.02 (d, 1H), 8.40 (d, 1H), 7.31−7.25 (m, 2H), 7.22−7.14 (m, 2H), 6.69 (d, 1H, CH), 6.28 (dt, 1H), 6.20−6.11 (m, 1H), 4.66 (s, 2H), 4.49−4.39 (m, 4H), 4.25−4.15 (m, 2H), 3.88−3.76 (m, 6H), 2.89−2.84 (m, 4H), 2.31−2.04 (m, 5H).

*19,21-Etheno-3-methyl-11-(2-(pyrrolidin-1-yl)ethoxy)-14-oxa-5,7,19,25-tetraaza-tetracyclo[18.3.1.1(2,6).1(8,12)]hexacosa-1-(24),2(25),3,5,8(26),9,11,16,20,22-decaene (14b).* The title compound was synthesized from **12b** (yield, 44%; >95% trans by ^{1}H NMR). LC-MS (ESI positive mode) $m/z$ 492 ([M + H]$^+$); ^{1}H NMR (MeOD-$d_4$) $\delta$ 8.80 (d, 1H), 8.32 (d, 1H), 7.83 (d, 1H), 7.31−7.28 (m, 2H), 7.18 (d, 1H), 7.07 (d, 1H), 6.31−6.17 (m, 2H), 4.56−4.47 (m, 4H), 4.36−4.24 (m, 4H), 4.04−3.95 (m, 2H), 3.82−3.77 (m, 5H), 2.71 (s, 3H), 2.21−2.13 (m, 5H).

*11-(2-(Pyrrolidin-1-yl)ethoxy)-14,19-dioxa-5,7,23,26-tetraaza-tetracyclo[19.3.1.1(2,6).1(8,12)]heptacosa-1(25),2(26),3,5,8-(27),9,11,16,21,23-decaene (14c).* The title compound was synthesized from **12c** (yield, 48%; >95% trans by ^{1}H NMR). LC-MS (ESI positive mode) $m/z$ 453 ([M + H]$^+$); ^{1}H NMR (DMSO-$d_6$) $\delta$ 9.78 (s, 1H), 9.54 (br s 1H), 8.73 (d, 1H), 8.48 (d, 1H), 7.90 (d, 1H), 7.35 (d, 1H), 7.15 (s, 1H), 7.10−7.14 (m, 1H), 6.23 (dt, 1H), 6.10 (dt, 1H), 4.90 (d, 2H), 4.11−4.35 (m, 11H), 3.70−3.74 (m, 2H), 2.63 (brs, 3H).

*11-(2-(Pyrrolidin-1-yl)ethoxy)-14,20-dioxa-5,7,22,26-tetraaza-tetracyclo[19.3.1.1(2,6).1(8,12)]heptacosa-1(25),2(26),3,5,8-(27),9,11,16,21,23-decaene (14d).* The title compound was synthesized from **12d** (yield, 39%; >95% trans by ^{1}H NMR). LC-MS (ESI positive mode) $m/z$ 437 ([M + H]$^+$); ^{1}H NMR (DMSO-$d_6$) $\delta$ 9.40 (s, 1H), 8.48 (d, 1H), 8.40 (d, 1H), 7.46 (d, 1H), 7.16 (d, 1H), 7.0 (dd, 1H), 6.90 (d, 1H), 6.67 (d, 1H), 5.93 (dt, 1H,), 5.69 (dt, 1H), 4.52 (s, 2H), 4.04−4.07 (m, 2H), 3.97 (d, 2H), 3.62−3.90 (m, 2H), 3.44 (s, 2H), 3.33 (s, 3H), 3.06 (d, 2H), 2.08 (s, 3H).

*3-Methyl-11-(2-(pyrrolidin-1-yl)ethoxy)-14,20-dioxa-5,7,22,26-tetraaza-tetracyclo[19.3.1.1(2,6).1(8,12)]heptacosa-1(25),2-(26),3,5,8(27),9,11,16,21,23-decaene (14e).* The title compound was synthesized from **12e** (yield, 65%; >95% trans by ^{1}H NMR). LC-MS (ESI positive mode) $m/z$ 482 ([M + H]$^+$); ^{1}H NMR (DMSO-$d_6$) $\delta$ 9.58 (s, 1H), 8.69 (m, 1H), 8.47 (m, 1H), 8.17 (s, 1H), 7.68 (m, 1H), 7.49−7.53 (m, 2H), 7.20 (m, 2H), 7.01 (m, 1H), 6.52 (m, 1H), 6.17 (m, 1H), 5.66 (m, 1H), 4.97 (m, 2H), 4.49 (m, 2H), 4.26 (m, 2H), 3.97 (m, 2H), 3.59−3.67 (m, 4H), 3.18 (m, 2H), 2.05 (m, 2H), 1.90 (m, 2H).

*12-Methyl-15-(2-(pyrrolidin-1-yl)ethoxy)-7,25-dioxa-12,19,21,24-tetraaza-tetracyclo[18.3.1.1(2,5).1(14,18)]hexacosa-1(24),2,4,9,14-(26),15,17,20,22-nonaene (14f).* The title compound was synthesized from **12f** (yield, 55%; >95% trans by ^{1}H NMR). LC-MS (ESI positive mode) $m/z$ 479 ([M + H]$^+$); ^{1}H NMR (MeOD-$d_4$) $\delta$ 8.66 (d, 1H), 8.32 (d, 1H), 7.81 (d, 1H), 7.27 (d, 1H), 7.12 (dd, 1H), 7.07−7.02 (m, 2H), 6.08 (dt, 1H), 5.98 (dt, 1H), 4.61 (s, 2H), 4.38 (t, 2H), 4.18 (d, 4H), 3.81 (br s, 2H), 3.69 (t, 2H), 3.37−3.35 (m, 2H), 2.22−2.08 (m, 6H).

*12-Methyl-15-(2-(pyrrolidin-1-yl)ethoxy)-7-oxa-25-thia-12,19,21,24-tetraaza-tetracyclo[18.3.1.1(2,5).1(14,18)]hexacosa-1-(24),2,4,9,14(26),15,17,20,22-nonaene (14g).* The title compound was synthesized from **12g** (yield, 70%; >95% trans by ^{1}H NMR). LC-MS (ESI positive mode) $m/z$ 479 ([M + H]$^+$); ^{1}H NMR (MeOD-$d_4$) $\delta$ 9.03 (d, 1H), 8.86 (d, 1H), 8.81 (d, 1H), 8.26 (s, 1H), 7.81 (d, 1H), 7.59 (dd, 1H), 7.56−7.51 (m, 1H), 6.38 (dt, 1H), 6.31 (dt, 1H), 5.24 (s, 2H), 5.14 (s, 2H), 4.86 (t, 2H), 4.65 (d, 2H), 4.54 (d, 2H), 4.29 (br s, 2H), 4.18 (t, 2H), 3.84−3.83 (m, 1H), 2.80−2.48 (m, 5H).

*15-(2-Methoxyethoxy)-12-methyl-7,25-dioxa-12,19,21,24-tetra-aza-tetracyclo[18.3.1.1(2,5).1(14,18)]hexacosa-1(24),2,4,9,14-(26),15,17,20,22-nonaene (14h).* The title compound was synthesized from **12h** (yield, 54%; >95% trans by ^{1}H NMR). LC-MS (ESI positive mode) $m/z$ 463 ([M + H]$^+$); ^{1}H NMR (MeOD-$d_4$) $\delta$ 8.56 (d, 1H), 8.38 (d, 1H), 8.29 (br s, 1H), 7.17 (d, 1H), 7.11−7.06 (m, 2H), 7.03−7.01 (m, 1H), 5.99 (dt, 1H), 5.84 (dt, 1H), 4.66 (s, 2H$_2$), 4.57 (s, 2H), 4.37 (t, 2H), 4.18 (d, 2H), 4.09 (d, 2H), 3.79 (brs, 2H), 3.69 (t, 2H), 3.35−3.34 (m, 2H), 2.21−2.07 (m, 4H).

*15-(2-(Pyrrolidin-1-yl)ethoxy)-7,12-dioxa-25-thia-19,21,24-triaza-tetracyclo[18.3.1.1(2,5).1(14,18)]hexacosa-1(24),2,4,9,14-(26),15,17,20,22-nonaene (14j).* The title compound was synthesized from **12j** (yield, 52%; >95% trans by $^1$H NMR). LC-MS (ESI positive mode) $m/z$ 463 ([M + H]$^+$); $^1$H NMR (MeOD-$d_4$) $\delta$ 8.51 (bs, 1H), 8.34 (bd, 1H), 7.75 (s, 1H), 7.49 (s, 1H), 7.11−7.06 (m, 2H), 7.00 (d, 1H), 6.07 (dt, 1H), 5.92 (dt, 1H), 4.63 (s, 2H), 4.47 (s, 2H), 4.36 (t, 2H), 4.19 (d, 2H), 4.08 (d, 2H), 3.79 (bs, 2H), 3.69 (t, 2H), 3.27−3.25 (m, 2H), 2.21−2.08 (m, 4H).

*15-(2-(Pyrrolidin-1-yl)ethoxy)-7,12-dioxa-4-thia-19,21,24-triaza-tetracyclo[18.3.1.1(2,5).1(14,18)]hexacosa-1(24),2,5(25),9,14-(26),15,17,20,22-nonaene (14k).* The title compound was synthesized from **12k** (yield, 34%; >95% trans by $^1$H NMR). LC-MS (ESI positive mode) $m/z$ 474 ([M + H]$^+$); $^1$H NMR (MeOD-$d_4$) $\delta$ 9.26 (brs, 1H), 8.90−8.87 (m, 2H), 8.61−8.58 (m, 2H), 7.44 (d, 1H), 7.15−7.12 (m, 1H), 7.06 (d, 1H), 5.96 (dt, 1H), 5.88 (dt, 1H), 4.77 (s, 2H), 4.64 (s, 2H), 4.38 (t, 2H), 4.15 (q, 4H), 3.81 (brs, 2H), 3.70 (t, 2H), 3.27−3.25 (m, 2H), 2.23−1.99 (m, 5H).

*(9E)-15-(2-(Pyrrolidin-1-yl)ethoxy)-7,12,25-trioxa-19,21,24-triaza-tetracyclo[18.3.1.1(2,5).1(14,18)]hexacosa-1(24),2,4,9,14(26), 15,17,20,22-nonaene (14l).* The title compound was synthesized from **12n** (yield, 46%; mixture of cis/trans 33:67 by $^1$H NMR). LC-MS (ESI positive mode) $m/z$ 474 ([M + H]$^+$); $^1$H NMR (MeOD-$d_4$) $\delta$ 8.91 (d, 1H), 8.57−8.54 (m, 1H), 8.28 (d, 1H), 7.70 (s, 1H), 7.51−7.46 (m, 1H), 7.38−7.32 (m, 1H), 7.14−7.12 (m, 1H), 7.05 (s, 1H), 5.93−5.85 (m, 1H), 5.68−5.62 (m, 1H), 4.46 (s, 2H), 4.58 (m, 2H), 4.46−4.34 (m, 2H), 4.12 (d, 2H), 3.82 (m, 2H), 3.72 (m, 2H), 3.37 (m, 2H), 2.52 (m, 2H), 2.25 (m, 2H), 2.10 (m, 2H).

*15-(2-(Pyrrolidin-1-yl)ethoxy)-4,7,12-trioxa-19,21,24-triaza-tetracyclo[18.3.1.1(2,5).1(14,18)]hexacosa-1(24),2,5(25),9,14-(26),15,17,20,22-nonaene (14m).* The title compound was synthesized from **12p** (yield, 58%; >95% trans by $^1$H NMR). LC-MS (ESI positive mode) $m/z$ 488 ([M + H]$^+$); $^1$H NMR (DMSO-$d_6$) $\delta$ 8.82 (d, 1H), 8.38 (s, 1H), 8.25 (d, 1H); 7.24−7.30 (m, 2H); 7.07−7.11 (m, 2H); 6.99−7.03 (m, 2H), 5.81−5.92 (m, 1H); 5.54−5.64 (m, 1H); 4.55−4.60 (m, 2H); 4.33−4.36 (m, 2H); 4.07 (d, 2H); 3.75−3.85 (m, 2H); 3.65−3.71 (m, 2H); 3.22−3.29 (m, 4H); 2.54−2.60 (m, 2H); 2.35 (s, 3H); 2.18−2.28 (m, 2H); 2.04−2.12 (m, 2H).

*15-(2-(Pyrrolidin-1-yl)ethoxy)-3,7,12-trioxa-19,21,24-triaza-tetracyclo[18.3.1.1(2,5).1(14,18)]hexacosa-1(24),2(25),4,9,14-(26),15,17,20,22-nonaene (14n).* The title compound was synthesized from **12q** (yield, 49%; >95% trans by $^1$H NMR). LC-MS (ESI positive mode) $m/z$ 496 ([M + H]$^+$); $^1$H NMR (MeOD-$d_4$) $\delta$ 8.54 (brs, 1H), 8.24 (s, 1H), 7.72 (s, 1H), 7.55 (d, 1H), 7.26 (d, 1H), 7.15 (d, 1H), 6.98 (dd, 1H), 6.88 (d, 1H), 6.44 (d, 1H), 5.96−6.01 (m, 1H), 5.37−5.43 (m, 1H), 4.85 (s, 2H), 4.39 (s, 2H), 4.20 (d, 2H), 3.90 (d, 2H), 3.65 (brs, 2H), 3.51 (d, 2H), 3.03−3.15 (m, 2H), 2.19 (s, 3H), 2.07 (brs, 2H), 1.92 (brs, 2H).

**Biology.** Enzyme assays (JAK1, JAK2, JAK3, TYK2, CDK2, and FLT3), cell proliferation, and computational algorithms were carried out as per the previously reported methods.[22,34] hERG activity was determined by MDS Pharma Services (www.mdsps.com). CYP induction and phenotyping was carried out at Cyprotex (www.cyprotex.com).

**Metabolic Stability in Liver Microsomes.** Reactions were carried out in a 96 well microtiter plate. Compound **14l** (5 $\mu$M) was incubated with HLM/MLM/DLM (at 0.87 mg/mL) or RLM and MoLM (at 1 mg/mL) in a reaction mix containing 50 mM potassium phosphate buffer (pH 7.4) and an NADPH regeneration system. The plate was incubated in an incubator shaker set at 37 °C. At predetermined time points, 0 min, 5,15, 30, 45, and 60 min, reactions (50 $\mu$L aliquots) were terminated by the addition of 100 $\mu$L of an ice-cold mixture of acetonitrile and DMSO (80:20, v/v).The terminated reaction mixtures were centrifuged and the supernatants analyzed by LC-MS. Stability was assessed by plotting the percent of parent compound remaining against time on a log−linear scale and estimating the half-life from the linear portion of the log−linear curve using the first order equation $t_{1/2} = 0.693/k$, where $k$ = slope of the curve (equal to the first order elimination rate constant).

**Human in Vitro CYP450 Inhibition Assay.** Compounds were incubated (at concentrations of 0.001, 0.01, 0.1, 1.0, 5, 10, and 25 $\mu$M) with human liver microsomes (0.25 mg/mL for CYP3A4 and 0.5 mg/mL for CYP1A2, CYP2C9, CYP2C19, and CYP2D6) and NADPH (1 mM) in the presence of the probe substrates testosterone for CYP3A4, phenacetin (CYP1A2), diclofenac (CYP2C9), omeprazole (CYP2C19), and dextromethorphan (CYP2D6) at 37 °C. The selective inhibitors ketoconazole, furafylline, sulphaphenazole, ticlopidine, and quinidine were used as positive controls for CYP3A4, 1A2, CYP2C9, CYP2C19, and CYP2D6, respectively. For all CYP enzymes, the reactions were terminated by the addition of a mixture of acetonitrile and DMSO (8:2). The samples were centrifuged, and the supernatants were analyzed for respective metabolites 6-$\beta$-hydroxytestosterone (CYP3A4), acetaminophen (CYP1A2), 4-hydroxydiclofenac (CYP2C9), 5-hydroxyomeprazole (CYP2C19), and dextrorphan (CYP2D6) by LC-MS/MS. Formic A decrease in the formation of the metabolites compared to the vehicle control was used to calculate an IC$_{50}$ value (test compound concentration which produces 50% inhibition).

**Caco-2 Bidirectional Permeability Assay.** Caco-2 cells obtained from ATCC were used between passage numbers 40−60. Cells were seeded on to Millipore Multiscreen Caco-2 plates at $1 \times 10^5$ cells/cm$^2$. The permeability study was performed on day 20. The incubation medium used was Hanks Balanced Salt Solution (HBSS) at pH 7.4, with 25 mM HEPES and 4.45 mM glucose at 37 °C. Incubations were carried out for 120 min in an atmosphere of 5% CO$_2$ with a relative humidity of 95% at 37 °C. The compound solutions were made by diluting 10 mM **14l** in DMSO with HBSS to give a final concentration of 10 $\mu$M (final DMSO concentration 1%). The apical compartment inserts were placed into companion plates containing fresh HBSS. For basolateral to apical (B→A) permeability determination, the experiment was initiated by replacing the buffer in the inserts, then placing them in companion plates containing dosing solutions. After 120 min, the companion plate was removed, and apical and basolateral samples were diluted and analyzed by LC-MS/MS. The permeability of **14l** was assessed in duplicate. On each plate, reference compounds of known permeability characteristics were run as controls. The control compound and **14l** were quantified by LC-MS/MS. The integrity of the monolayers throughout the experiment was checked by monitoring lucifer yellow permeation using fluorimetric analysis.

**In Vitro Plasma Protein Binding.** Equilibrium dialysis was performed in a Micro-Equilibrium Dialyzer (Harvard Apparatus) with a chamber volume of 500 $\mu$L (each compartment with a volume of 250 $\mu$L). The semipermeable membrane used was rinsed with Milli-Q-water and soaked for 10 min in PBS. Compound **14l** was added to plasma (from mouse, rat, dog, monkey, and humans) to obtain a final concentration of 1000 ng/mL. The spiked plasma was vortexed, and 250 $\mu$L was aliquoted into one chamber of the dialyzer cell. The other chamber was filled with 250 $\mu$L of PBS buffer. The assembled cell was placed into a water-bath at 37 °C, and dialysis was performed for 4 h. Following dialysis, 50 $\mu$L of PBS dialyzed samples containing free **14l** was transferred into 2 mL Eppendorf tubes in triplicate for extraction. Samples were extracted with 1250 $\mu$L of MTBE (methyl tertiary-butyl ether) for 30 min and centrifuged at 4 °C for 10 min at 13,000 rpm in a microcentrifuge. The supernatants (1000 $\mu$L) were transferred into fresh Eppendorf tubes and dried in a SpeedVac at 43 °C for 35 min. The dried samples were reconstituted with 100 $\mu$L of acetonitrile/ Milli-Q-water (60:40), vortexed, centrifuged for 2 min at 13,000 rpm, and analyzed by LC-MS/MS.

**Pharmacokinetics.** Female BALB/c nude mice (aged 8−10 weeks and weighing 18−22 g), male Wistar rats (aged 8−10 weeks, weighing 230−260 g), male Beagle dogs (∼5−6 months of age, weighing ∼10 kg), and male rhesus monkeys (∼4 years of age and weighing 6−7 kg) were used in the studies. All the animal studies were performed as per approved internal protocols for animal care and use. The oral doses for mice, rats, dogs, and monkeys were 50, 50, 5, and 20 mg/kg, respectively. The doses were administered, by gavage, as suspensions (0.5% methylcellulose and 0.1% Tween 80) to mice, rats, and monkeys and as gelatin capsules (SNAP-FIT, Capsugel) to dogs. Following oral dosing, serial blood samples were collected at different time points (0 to 24 h) in tubes containing K$_3$EDTA as anticoagulant and centrifuged, and plasma was separated and stored at −70 °C until analysis. Plasma samples were processed and analyzed by LC/MS/MS.

Pharmacokinetic parameters were estimated by noncompartmental methods using WinNonlin (ver 5.2, Pharsight, CA).

**High Throughput Solubility Assay.** This assay measures the solubility of a compound in PBS in a high throughput mode. The assay was done using 96-well semitransparent PP microplates with a V-shaped bottom (Greiner Bio-one) and 96-well UV transparent microplates (Greiner Bio-One). Compound solutions (250 $\mu$M) were prepared in 10 mM phosphate buffer (pH 7.0) containing 20% DMSO in a total volume of 0.2 mL. Plates were placed on a shaker set at 600 rpm for 1.5 h, following which the plates were allowed to stand for 2 h at room temperature. The plates were centrifuged at 1500g for 15 min. The supernatants were transferred to a UV transparent microplate and analyzed by UV-spectrophotometry at the appropriate absorption maxima. The concentration of the compound in the supernatant was quantified using a calibration curve.

**Thermodynamic Solubility Assay.** This assay measures the solubility of a compound in pH buffered solutions in a low throughput mode with HPLC quantification. Approximately 5 mg of **14l** (citrate) was weighed into individual 4 mL glass vials. Appropriate volumes of buffers of pH 1, 3, 5, 7, and 9 were added to corresponding vials containing the compound to make 5 mg/mL (w/v) stock of **14l**. Each sample was made in triplicate. Prior to the addition of buffers, their initial pH was recorded. Following addition of the buffers, the vials were capped tightly with screw caps, transferred to the shaking platform, and allowed to shake for 24 h at 600 rpm at room temperature. After 24 h of shaking, each sample was filtered using a syringe filter (0.4 $\mu$m) into clean Eppendorf tubes, and final pH of the filtrate was measured. The filtrates were appropriately diluted using acetonitrile/water (1:1), vortexed for 3 min, and centrifuged at 13200 rpm for 3 min. The resultant supernatant was transferred into HPLC vials and analyzed by HPLC-UV.

**Cell Lines.** SET2 cells were obtained from DSMZ (Braunschweig, Germany), while HL60, MDA-MB-231, HEK293, and 32D cells were obtained from the American Type Culture Collection (ATCC, Manassas, VA). These cells were cultured as described previously.[34] Human CD4+ T cells, isolated from peripheral blood mononuclear cells with >95% purity, were purchased from AllCells (Emeryville, CA) and maintained in X-VIVO 20 media (Lonza, Basel, Switzerland).

**Western Blot Analyses.** Cells were lysed and proteins immunoprecipitated as previously described.[34] Following SDS–polyacrylamide gel electrophoresis, proteins were transferred to PVDF membranes. Western blots were performed according to standard methods. pJAK2 (Y1007/8) (Cat #3776), pSTAT3 (Y705), antimouse IgG (Cat #7074), and antirabbit IgG, HRP-linked (Cat #7076) antibodies were purchased from Cell Signaling Technology (Beverly, MA). pSTAT4 (Y693) (Cat# AF4319) was from R&D systems (Minneapolis, MN). pSTAT5 (Y694, Cat #611965) was obtained from BD Biosciences (San Jose, CA), tubulin (Cat #65–829) from Millipore (Billerica, MA), and actin (Cat #A2066) from Sigma (St Louis, MO). After the final wash, membranes were incubated for 5 min in ECL from GE-Healthcare (Singapore). The images were captured digitally using the LAS-3000 Life Science Imager from Fujifilm (Tokyo, Japan). Densitometric analysis was performed using MultiGauge software (v3.1) from Fujifilm.

**Collagen-Induced Arthritis (CIA).**[32,33] The mouse CIA study was performed at Bolder BioPATH (Boulder, CO) and was approved by the Bolder BioPATH's Institutional Animal Care and Use Committee (IACUC). Six to eight week old male B10/RIII mice were obtained from Jackson Laboratories (Bar Harbor, ME). The mice were immunized by injecting 300 $\mu$g of bovine type II collagen (Elastin Products, Owensville, MO) emulsified in Freund's Complete Adjuvant (Sigma) at the base of the tail on day 0 and again on day 15. The mice were randomized into treatment groups, and oral treatment with **14l** was initiated after the onset of arthritis (usually between days 18–22) identified by establishment of swelling in at least one paw. Treatment was continued twice daily (b.i.d) for 10 days. Arthritis severity was evaluated on a scale of 0–5 based on the number of joints affected, swelling of the joints, and the severity of erythema. The sum of scores for all four paws from each mouse was used as the total clinical score. The data for paw scores (mean for animal) was analyzed by determining the area under the dosing curve (AUC). The daily mouse scores were obtained, and the area under the curve between the treatment days and the final day was computed. Means for each group were determined, and percentage inhibition from arthritis controls was calculated by comparing values for treated and normal animals.

## ASSOCIATED CONTENT

**⑤ Supporting Information**

## AUTHOR INFORMATION

**Corresponding Author**
*Tel: +65 62195443. E-mail: wanthony11@yahoo.com.

**Notes**

## ACKNOWLEDGMENTS

## ABBREVIATIONS USED

CIA, collagen induced arthritis; CDKs, cyclin-dependent kinases; CYP, cytochrome P450; FLT3, fms-like tyrosine kinase 3; JAK2, janus kinase 2; RA, rheumatoid arthritis; RCM, ring closing metathesis; STAT, signal transducer and activator of transcription; TYK2, tyrosine kinase 2

## REFERENCES

(1) Walsh, N. C.; Gravallese, E. M. Bone remodeling in rheumatic disease: a question of balance. *Immunol. Rev.* **2010**, *233*, 301−312.

(2) Machold, K. P.; Nell, V. P.; Stamm, T. A.; Smolen, J. S. Aspects of early arthritis. Traditional DMARD therapy: is it sufficient? *Arthritis Res. Ther.* **2006**, *8*, 211.

(3) Wong, M.; Ziring, D.; Korin, Y.; Desai, S.; Kim, S.; Lin, J.; Gjertson, D.; Braun, J.; Reed, E.; Singh, R. R. TNFalpha blockade in human diseases: mechanisms and future directions. *Clin. Immunol.* **2008**, *126*, 121−136.

(4) Khraishi, M. Comparative overview of safety of the biologics in rheumatoid arthritis. *J. Rheumatol. Suppl.* **2009**, *82*, 25−32.

(5) Buch, M. H.; Emery, P. New therapies in the management of rheumatoid arthritis. *Curr. Opin. Rheumatol.* **2011**, *23*, 245−251.

(6) Walker, J. G.; Smith, M. D. The Jak-STAT pathway in rheumatoid arthritis. *J. Rheumatol.* **2005**, *32*, 1650−1653.

(7) Yamaoka, K.; Saharinen, P.; Pesu, M.; Holt, V. E. T.; Silvennoinen, O.; O'Shea, J. J. The Janus kinases (Jaks). *Genome Biol.* **2004**, *5*, 253.1−253.6.

(8) Wang, T.; Duffy, J. P.; Wang, J.; Halas, S.; Salituro, F. G.; Pierce, A. C.; Zuccola, H. J.; Black, J. R.; Hogan, J. K.; Jepson, S.; Shlyakter, D.; Mahajan, S.; Gu, Y.; Hoock, T.; Wood, M.; Furey, B. F.; Frantz, J. D.; Dauffenbach, L. M.; Germann, U. A.; Fan, B.; Namchuk, M.; Bennani, Y. L.; Ledeboer, M. W. Janus kinase 2 inhibitors. Synthesis and characterization of a novel polycyclic azaindole. *J. Med. Chem.* **2009**, *52*, 7938−7941.

(9) Chen, A. T.; Prchal, J. T. JAK2 kinase inhibitors and myeloproliferative disorders. *Curr Opin Hematol* **2010**, *17*, 110−116.

(10) Flanagan, M. E.; Blumenkopf, T. A.; Brissette, W. H.; Brown, M. F.; Casavant, J. M.; Chang, S.-P.; Doty, J. L.; Elliott, E. A.; Fisher, M. B.; Hines, M.; Kent, C.; Kudlacz, E. M.; Lillie, B. M.; Magnuson, K. S.; McCurdy, S. P.; Munchhof, M. J.; Perry, B. D.; Sawyer, P. S.; Strelevitz, T. J.; Subramanyam, C.; Sun, J.; Whipple, D. A.; Changelian, P. S.

Discovery of CP-690,550: A potent and selective Janus kinase (JAK) inhibitor for the treatment of autoimmune diseases and organ transplant rejection. *J. Med. Chem.* **2010**, *53*, 8468–8484.

(11) Fridman, J. S.; Scherle, P. A.; Collins, R.; Burn, T. C.; Li, Y.; Li, J.; Covington, M. B.; Thomas, B.; Collier, P.; Favata, M. F.; Wen, X.; Shi, J.; McGee, R.; Haley, P. J.; Shepard, S.; Rodgers, J. D.; Yeleswaram, S.; Hollis, G.; Newton, R. C.; Metcalf, B.; Friedman, S. M.; Vaddi, K. Selective inhibition of JAK1 and JAK2 is efficacious in rodent models of arthritis: preclinical characterization of INCB028050. *J. Immunol.* **2010**, *184*, 5298–5307.

(12) Kiss, R.; Sayeski, P. P.; Keserū, G. M. Recent developments on JAK2 inhibitors: a patent review. *Expert Opin. Ther. Pat.* **2010**, *20*, 471–495.

(13) Mesa, R. A. Ruxolitinib, a selective JAK1 and JAK2 inhibitor for the treatment of myeloproliferative neoplasms and psoriasis. *IDrugs* **2010**, *13*, 394–403.

(14) Passamonti, F.; Maffioli, M.; Caramazza, D. New generation small-molecule inhibitors in myeloproliferative neoplasms. *Curr. Opin. Hematol.* **2012**, *19*, 117–123.

(15) Santos, F. P.; Verstovsek, S. JAK2 inhibitors: What's the true therapeutic potential? *Blood Rev.* **2011**, *25*, 53–63.

(16) Quintas-Cardama, A.; Kantarjian, H.; Cortes, J.; Verstovsek, S. Janus kinase inhibitors for the treatment of myeloproliferative neoplasias and beyond. *Nat. Rev. Drug Discovery* **2011**, *10*, 127–140.

(17) Ioannidis, S.; Lamb, M. L.; Wang, T.; Almeida, L.; Block, M. H.; Davies, A. M.; Peng, B.; Su, M.; Zhang, H. J.; Hoffmann, E.; Rivard, C.; Green, I.; Howard, T.; Pollard, J.; Read, J.; Alimzhanov, M.; Bebernitz, G.; Bell, K.; Ye, M.; Huszar, D.; Zinda, M. Discovery of 5-chloro-N2-[(1S)-1-(5-fluoropyrimidin-2-yl)ethyl]-N4-(5-methyl-1H-pyrazol −3-yl)pyrimidine-2,4-diamine (AZD1480) as a novel inhibitor of the Jak/Stat pathway. *J. Med. Chem.* **2011**, *54*, 262–276.

(18) Paunovic, V.; Carroll, H. P.; Vandenbroeck, K.; Gadina, M. Signalling, inflammation and arthritis: crossed signals: the role of interleukin (IL)-12, −17, −23 and −27 in autoimmunity. *Rheumatology (Oxford)* **2008**, *47*, 771–776.

(19) Ishizaki, M.; Muromoto, R.; Akimoto, T.; Ohshiro, Y.; Takahashi, M.; Sekine, Y.; Maeda, H.; Shimoda, K.; Oritani, K.; Matsuda, T. Tyk2 deficiency protects joints against destruction in anti-type II collagen antibody-induced arthritis in mice. *Int. Immunol.* **2011**, *23*, 575–582.

(20) Dehlin, M.; Bokarewa, M.; Rottapel, R.; Foster, S. J.; Magnusson, M.; Dahlberg, L. E.; Tarkowski, A. Intra-articular fms-like tyrosine kinase 3 ligand expression is a driving force in induction and progression of arthritis. *PLoS One* **2008**, *3*, e3633.

(21) Dehlin, M.; Andersson, S.; Erlandsson, M.; Brisslert, M.; Bokarewa, M. Inhibition of fms-like tyrosine kinase 3 alleviates experimental arthritis by reducing formation of dendritic cells and antigen presentation. *J. Leukocyte Biol.* **2011**, *90*, 811–817.

(22) William, A. D.; Lee, A. C.; Blanchard, S.; Poulsen, A.; Teo, E. L.; Nagaraj, H.; Tan, E.; Chen, D.; Williams, M.; Sun, E. T.; Goh, K. C.; Ong, W. C.; Goh, S. K.; Hart, S.; Jayaraman, R.; Pasha, M. K.; Ethirajulu, K.; Wood, J. M.; Dymock, B. W. Discovery of the macrocycle 11-(2-pyrrolidin-1-yl-ethoxy)-14,19-dioxa-5,7,26-triaza-tetracyclo[19.3.1.1(2,6).1(8,12)]heptacosa-1(25),2(26),3,5,8,10,12(27),16,21,23-decaene (SB1518), a potent Janus kinase 2/fms-like tyrosine kinase-3 (JAK2/FLT3) inhibitor for the treatment of myelofibrosis and lymphoma. *J. Med. Chem.* **2011**, *54*, 4638–4658.

(23) William, A. D.; Lee, A.; Goh, K. C.; Blanchard, S.; Poulsen, A.; Teo, E.; Nagaraj, H.; Lee, C. P.; Wang, H.; Williams, M.; Sun, E. T.; Hu, C.; Jayaraman, R.; Pasha, M. K.; Ethirajulu, K.; Wood, J.; Dymock, B. W. Discovery of kinase spectrum selective macrocycle (16E)-14-Methyl-20-oxa-5,7,14,26-tetraaza-tetracyclo[19.3.1.1(2,6).1(8,12)]-heptacosa-1(25),2(26),3,5,8(27),9,11,16,21,23-decaene (SB1317/TG02), a potent inhibitor of cyclin dependant kinases (CDKs), Janus kinase 2 (JAK2) and Fms-liketyrosine kinase-3 (FLT3) for the treatment of cancer. *J. Med. Chem.* **2012**, *55*, 169–196.

(24) Cai, Q.; Zhao, Z.-A.; You, S.-L. Asymmetric construction of polycyclic indoles through olefin cross- metathesis/intramolecular

Friedel−Crafts alkylation under sequential catalysis. *Angew. Chem., Int. Ed.* **2009**, *48*, 7428–7431.

(25) Schmidt, B. Ruthenium-catalyzed cyclizations: more than just olefin metathesis! *Angew. Chem., Int. Ed.* **2003**, *42*, 4996–4999.

(26) Chen, L. J.; DeRose, E. F.; Burka, L. T. Metabolism of furans in vitro: ipomeanine and 4-ipomeanol. *Chem. Res. Toxicol.* **2006**, *19*, 1320–1329.

(27) Lu, D.; Peterson, L. A. Identification of furan metabolites derived from cysteine-cis-2-butene-1,4-dial-lysine cross-links. *Chem. Res. Toxicol.* **2010**, *23*, 142–151.

(28) Lant, M. S.; Martin, L. E.; Oxford, J. Qualitative and quantitative analysis of ranitidine and its metabolites by high-performance liquid chromatography-mass spectrometry. *J. Chromatogr.* **1985**, *323*, 143–152.

(29) Madan, B.; Goh, K. C.; Hart, S.; William, A. D.; Jayaraman, R.; Ethirajulu, K.; Dymock, B. W.; Wood, J. M., unpublished results.

(30) Wang, S.; Fischer, P. M. Cyclin-dependent kinase 9: a key transcriptional regulator and potential drug target in oncology, virology and cardiology. *Trends Pharmacol. Sci.* **2008**, *29*, 302–13.

(31) Quentmeier, H.; MacLeod, R. A.; Zaborski, M.; Drexler, H. G. JAK2 V617F tyrosine kinase mutation in cell lines derived from myeloproliferative disorders. *Leukemia* **2006**, *20*, 471–476.

(32) Holmdahl, R.; Andersson, M. E.; Goldschmidt, T. J.; Jansson, L.; Karlsson, M.; Malmström, V.; Mo, J. Collagen induced arthritis as an experimental model for rheumatoid arthritis. Immunogenetics, pathogenesis and autoimmunity. *APMIS* **1989**, *97*, 575–584.

(33) Williams, R. O. Collagen-induced arthritis as a model for rheumatoid arthritis. *Methods Mol. Med.* **2004**, *98*, 207–216.

(34) Hart, S.; Goh, K. C.; Novotny-Diermayr, V.; Hu, C. Y.; Hentze, H.; Tan, Y. C.; Madan, B.; Amalini, C.; Loh, Y. K.; Ong, L. C.; William, A. D.; Lee, A.; Poulsen, A.; Jayaraman, R.; Ong, K. H.; Ethirajulu, K.; Dymock, B. W.; Wood, J. W. SB1518, a novel macrocyclic pyrimidine-based JAK2 inhibitor for the treatment of myeloid and lymphoid malignancies. *Leukemia* **2011**, *25*, 1751–1759.